

**DESIGN OF 3.5 GHZ BANDPASS PARALLEL – COUPLED
MICROSTRIP LINE FILTER FOR THE 5G NEW RADIO**

İsmail Oğuz Saylan
091405201

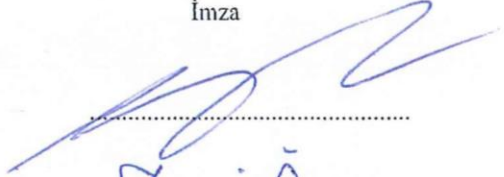


MASTER THESIS

Department of Electrics-Electronics Engineering
Electrics-Electronics Engineering Program
Advisor: Assoc. Prof. Dr. Serkan Topaloğlu

İstanbul
T.C. Maltepe University
Graduate School of Science and Engineering
July, 2019

JÜRİ VE ENSTİTÜ ONAYI

İSMAİL OĞUZ SAYLAN'ın "Design of 3.5 GHz Bandpass Parallel-Coupled Microstrip Line Filter For The 5G New Radio" başlıklı tezi 12.07.2019 tarihinde aşağıdaki jüri tarafından değerlendirilerek "Maltepe Üniversitesi Lisansüstü Eğitim ve Öğretim Yönetmeliği" nin ilgili maddeleri uyarınca Elektrik-Elektronik Mühendisliği Anabilim Dalı Yüksek Lisans/~~Doktora~~ tezi oy birliğiyle/~~oy çokluğuyla~~, başarılı/~~başarısız~~ olarak kabul edilmiştir.

	Unvanı, Adı ve Soyadı	İmza
Üye (Tez Danışmanı)	Doç. Dr. Serkan TOPALOĞLU	
Üye	Dr. Öğr. Üyesi Burhan Demir ÖNER	
Üye	Dr. Öğr. Üyesi Ali AKMAN	



Prof. Dr. İlter BÜYÜKDIĞAN
Enstitü Müdürü



ŞEKİL ONAY SAYFASI

Doküman No	FR-105
İlk Yayın Tarihi	20.12.2017
Revizyon Tarihi	10.12.2018
Revizyon No	01
Sayfa	1/2

ŞEKİL ONAY SAYFASI

25/07/2019

FEN BİLİMLERİ ENSTİTÜSÜ MÜDÜRLÜĞÜNE,

Aşağıda bilgileri bulunan lisansüstü öğrencinin tezi şekil yönünden tarafımda incelenmiş ve Enstitüye teslim edilmesi uygun bulunmuştur.

Anabilim Dalı Başkanı
Dr. Öğr. Üyesi Burhan Demir ÖNER

ÖĞRENCİ BİLGİLERİ

ADI SOYADI	İsmail Oğuz SAYLAN
ÖĞRENCİ NUMARASI	091405201
ANABİLİM DALI	Elektrik - Elektronik Mühendisliği Anabilim Dalı
PROGRAMI	(X) YÜKSEK LİSANS () DOKTORA () SANATTA YETERLİK
DANIŞMANI	Doç. Dr. Serkan TOPALOĞLU
TEZ BAŞLIĞI	DESIGN OF 3.5 GHZ BANDPASS PARALLEL – COUPLED MICROSTRIP LINE FILTER FOR THE 5G NEW RADIO
SAVUNMA TARİHİ	12/07/2019
e-posta	iosaylan@hotmail.com

İç Kapak	<input checked="" type="checkbox"/> Var <input type="checkbox"/> Yok
Jüri Onay Sayfası	<input checked="" type="checkbox"/> Var <input type="checkbox"/> Yok
Etik İlke ve Kurallara Uyum Beyanı	<input checked="" type="checkbox"/> Var <input type="checkbox"/> Yok
İntihal Raporu	<input checked="" type="checkbox"/> Var <input type="checkbox"/> Yok
Teşekkür Sayfası	<input checked="" type="checkbox"/> Var <input type="checkbox"/> Yok
Öz (Başlık-Öz-Anahtar Sözcükler)	<input checked="" type="checkbox"/> Var <input type="checkbox"/> Yok
Abstract (Title-Abstract-Key Words)	<input checked="" type="checkbox"/> Var <input type="checkbox"/> Yok
İçindekiler	<input checked="" type="checkbox"/> Var <input type="checkbox"/> Yok
Çizelgeler Listesi	<input type="checkbox"/> Var <input checked="" type="checkbox"/> Yok
Şekiller Listesi (varsa)	<input type="checkbox"/> Şekil yok <input checked="" type="checkbox"/> Uygundur <input type="checkbox"/> Uygun Değildir
Kısaltmalar Listesi	<input checked="" type="checkbox"/> Var <input type="checkbox"/> Yok
Tablolar Listesi (varsa)	<input type="checkbox"/> Tablo yok <input checked="" type="checkbox"/> Uygundur <input type="checkbox"/> Uygun Değildir
Ekler Listesi (varsa)	<input checked="" type="checkbox"/> Ek yok <input type="checkbox"/> Uygundur <input type="checkbox"/> Uygun Değildir

Hazırlayan
İlgili Birim

Kalite Koordinatörü
Dr. Öğr. Üyesi Şafak GÜNDÜZ

Kurumsal Yetkili
Prof. Dr. Belma AKŞİT



ŞEKİL ONAY SAYFASI

Doküman No	FR-105
İlk Yayın Tarihi	20.12.2017
Revizyon Tarihi	10.12.2018
Revizyon No	01
Sayfa	2/2

Özgeçmiş	<input checked="" type="checkbox"/> Var <input type="checkbox"/> Yok
Sayfa Genişliği	<input checked="" type="checkbox"/> Uygundur <input type="checkbox"/> Uygun Değildir
Yazı Tipi	<input checked="" type="checkbox"/> Uygundur <input type="checkbox"/> Uygun Değildir
Referans Kullanımı	<input checked="" type="checkbox"/> Uygundur <input type="checkbox"/> Uygun Değildir
Kaynakça Yazımı	<input checked="" type="checkbox"/> Uygundur <input type="checkbox"/> Uygun Değildir
Ekler (varsa)	<input checked="" type="checkbox"/> Ek yok <input type="checkbox"/> Uygundur <input type="checkbox"/> Uygun Değildir

Dr. Öğr. Üyesi Erdal GÜVENOĞLU

Hazırlayan
İlgili Birim

Kalite Koordinatörü
Dr. Öğr. Üyesi Şafak GÜNDÜZ

Kurumsal Yetkili
Prof. Dr. Belma AKŞİT

 maltepe üniversitesi	ETİK İLKE VE KURALLARA UYUM BEYANI	Doküman No	FR-178
		İlk Yayın Tarihi	01.03.2018
		Revizyon Tarihi	
		Revizyon No	00
		Sayfa	1/1

Revizyon Takip Tablosu

REVİZYON NO	TARİH	AÇIKLAMA
00	01.03.2018	İlk yayın.

ETİK İLKE VE KURALLARA UYUM BEYANI

12/07/2019

Bu tezin bana ait, özgün bir çalışma olduğunu; çalışmamın hazırlık, veri toplama, analiz ve bilgilerin sunumu olmak üzere tüm aşamalarından bilimsel etik ilke ve kurallara uygun davrandığımı; bu çalışma kapsamında elde edilmeyen tüm veri ve bilgiler için kaynak gösterdiğimi ve bu kaynaklara kaynakçada yer verdiğimi; çalışmamın Maltepe Üniversitesinde kullanılan "bilimsel intihal tespit programı" ile tarandığını ve öngörülen standartları karşıladığını beyan ederim.

Herhangi bir zamanda, çalışmamla ilgili yaptığım bu beyana aykırı bir durumun saptanması durumunda, ortaya çıkacak tüm ahlaki ve hukuki sonuçlara razı olduğumu bildiririm.



İsmail Oğuz SAYLAN

Hazırlayan İlgili Birim	Kalite Koordinatörü Dr. Öğr. Üyesi Şafak GÜNDÜZ	Kurumsal Yetkili Prof. Dr. Belma AKŞİT
----------------------------	--	---

(Doküman No: FR-178; Yayın Tarihi: 01.03.2018; Revizyon Tarihi: ; Revizyon No:00)

DESIGN OF 3.5 GHZ BANDPASS PARALLEL – COUPLED MICROSTRIP LINE FILTER FOR THE 5G NEW RADIO

ORIJINALLIK RAPORU

%21
BENZERLIK ENDEKSI

%11
İNTERNET
KAYNAKLARI

%10
YAYINLAR

%18
ÖĞRENCİ ÖDEVLERİ

BİRİNCİL KAYNAKLAR

- 1** Submitted to Universiti Teknikal Malaysia Melaka
Öğrenci Ödevi %1
- 2** Submitted to University of Bradford
Öğrenci Ödevi %1
- 3** is.muni.cz
İnternet Kaynağı %1
- 4** Submitted to Universiti Teknologi Malaysia
Öğrenci Ödevi %1
- 5** Submitted to Higher Education Commission Pakistan
Öğrenci Ödevi %1
- 6** Submitted to University of Birmingham
Öğrenci Ödevi %1
- 7** www.ukessays.com
İnternet Kaynağı <%1
- 8** www.slideshare.net

ACKNOWLEDGEMENTS

In conducting my master thesis;

First of all, I would like to thank my esteemed advisor Assoc. Prof. Dr. Serkan TOPALOĞLU who guided me with his knowledge and experience and always supported my work in a patient and willing manner.

I would like to thank to my teachers who have contributed to my education with their knowledge and experience during my Master of Science education and to Umutcan KORKMAZ (Yeditepe University - Electrical and Electronics Engineering Graduate Scholar) for his assistance in measurement.

I would like to express my thanks to my team leader and my colleagues at Huawei R&D Center for their understanding during this process.

Lastly, I would like to thank my wife, Seda SAYLAN, who motivated me patiently for my work and lend considerable support to me in all circumstances; my beloved daughter Ece SAYLAN for her consideration; my parents (Nevin – Şerif SAYLAN) and my sister (Ayşe Zeynep SAYLAN DALMAN) for their everlasting support.

İsmail Oğuz Saylan

July 2019

ÖZ

5G YENİ RADYO İÇİN 3.5 GHZ BANT GEÇİREN PARALEL KUPLAJLI MİKROŞERİT FİLTRE TASARIMI

İsmail Oğuz Saylan

Yüksek Lisans Tezi

Elektrik - Elektronik Mühendisliği Anabilim Dalı

Elektrik - Elektronik Mühendisliği Programı

Danışman: Doç. Dr. Serkan Topaloğlu

Maltepe Üniversitesi Fen Bilimleri Enstitüsü, 2019

Filtreler, elektronik sistemlerde önemini ve gerekliliğini korumakta ve son yıllarda yeni teknolojilerin ortaya çıkmasındaki hız ile birlikte filtre talepleri artmaktadır. Haberleşme sistemindeki yeni teknolojilerden birisi 5G'dir. Haberleşme sisteminde ortaya çıkan her yeni teknoloji ile birlikte, mevcut frekans bantlarının kullanımı artmış veya yeni frekans bant tahsisleri yapılmıştır. Yeni frekans dağılımlarının bir sonucu olarak, birbirine çok yakın bitişik frekans bantları meydana gelmektedir.

Filtreler, taşınan sinyale girişimi önlemek için iletişim sistemlerinin temel parçasıdır. Alçak geçiren, yüksek geçiren, bant geçiren veya bant durduran, haberleşme sistemlerinde kullanılan farklı filtre tipleridir. Bant geçiren filtre, belirli bir frekans aralığındaki sinyali iletmek ve bu aralığın dışındaki sinyalleri söndürmek için kullanılabilir. Frekans bandı veya filtrenin kullanılacağı uygulamaya göre, filtre teknolojisi seçilebilir. Toplu elemanlı filtreler kompakt tasarımlar için pratik değil ve yüksek frekanslarda güvenilir değildir, çünkü sinyalin dalga boyu devrenin fiziksel boyutlarından çok daha küçüktür. Dağılmış elemanlı filtre; yüksek dielektrik sabitiyle yüksek frekanslı uygulamalar için kullanılabilir, düşük kayıplıdır ve haberleşme sistemlerinde filtre topolojisine göre iletim hatlarına uygulanması kolaydır.

Bu yüksek lisans tez çalışmasında, paralel kuplajlı mikro şerit bant geçiren filtre, 5G (n78 bant; 3400 MHz – 3600 MHz) uygulamalarında taşınan sinyallere bitişik bantlardan gelen girişimleri önlemek için tasarlandı, simüle edildi, optimize edildi ve gerçekleştirildi. Tasarımda ve filtrenin gerçekleştirilmesinde, dielektrik sabitli $\epsilon_r = 3.48$ RO4350 (Rogers) alt katman malzemesi olarak seçildi. Filtre tasarımında, geçiş bandında 0.5 dB dalgalanmalı Chebyshev alçak geçiren filtre prototipi kullanıldı. Beşinci derece paralel kuplajlı mikro şerit bant geçiren filtre, 200 MHz bant genişliği ve merkezi frekans 3.5 GHz ile tasarlanmıştır. Simülasyon sonuçlarına göre; 3.5 GHz merkez frekansında araya girme kaybı $s_{21} = -3.49$ dB geri dönüş kaybı $s_{11} = -16.94$ dB' dir ve -3 dB

bant genişliđi, üst ve alt kesim frekansların sırasıyla 3617 MHz ve 3418 MHz olduđu 199 MHz' dir. Bant durdurma bastırması, 3.3 GHz' de -33.33 dB ve 3.8 GHz' de -50.81 dB' dir. Tasarlanan filtre gerçeklendi ve ölçüldü; 3.5 GHz merkez frekansında araya girme kaybı $s_{21} - 3.23$ dB, geri dönüş kaybı $s_{11} - 27.84$ dB' dir ve -3 dB bant genişliđi, üst ve alt frekansların sırasıyla 3615 MHz ve 3382 MHz olduđu 233 MHz' dir. Bant durdurma bastırması, 3.3 GHz' de -22.45 dB ve 3.8 GHz' de -41.99 dB' dir. Gerçeklenen filtrenin ölçümü ve tasarlanan filtre simülasyonu, filtre cevabında benzer sonuçlara sahiptir. Tasarlanan filtre gerçeklendi ve sonuçta düşük araya girme kaybı, düşük gerçekleştirme maliyeti ve yüksek söndürme özelliđi elde edildi. Tasarlanan filtrenin uygulama alanı boyutlarında herhangi bir sınırlama yoksa, bu gerçekenmiş filtre, düşük maliyetli çözümler için avantaj sağlar.

Anahtar Sözcükler: 1. Mikro şerit; 2. Bant geçiren filtre; 3. 5G NR Frekans bandı; 4. Paralel kuplajlı



ABSTRACT

DESIGN OF 3.5 GHZ BANDPASS PARALLEL – COUPLED MICROSTRIP LINE FILTER FOR THE 5G NEW RADIO

İsmail Oğuz Saylan

Master Thesis

Department of Electrics-Electronics Engineering

Electrics-Electronics Engineering Program

Advisor: Assoc. Prof. Dr. Serkan Topaloğlu

Maltepe University, Institute of Science and Technology, 2019

Filters maintain their importance and necessity in electronic systems and filter demands are increased in recent years due to speed of emerging new technologies. One of the new technologies in communication system is 5G. With every new technology emerged in communication systems, existing frequency bands usage increases or new frequency band allocations are made. As a result of new frequency allocations, very close each other adjacent frequency bands are occurring.

The filters are the essential part of communication systems to prevent transporting signal from interference. Different type of filters; low pass, high pass, bandpass or bandstop are used in communication systems. The bandpass filter can be used to pass signals in a specific frequency range and to attenuate signals out of this range. According to frequency band or application which filter will be used, filter technology can be chosen. Lumped element filters are not practical for compact designs and not reliable in high frequencies because the wavelength of the signal is much smaller than the physical dimensions of the circuit. Distributed element filter; can be used for high frequency applications with high dielectric constant, is low loss and easy to implement to transmission lines according to filter topology in communication systems.

In this master thesis, a parallel coupled microstrip bandpass filter is designed, simulated, optimized and realized for 5G (n78band; 3400 MHz – 3600 MHz) applications to prevent transporting signal from adjacent band interference. In the design and for filter realization, RO4350 (Rogers) with dielectric constant $\epsilon_r = 3.48$ is chosen as substrate material. In the filter design, 0.5 dB ripple in the passband Chebyshev low pass filter prototype is used. The 5th order parallel coupled microstrip bandpass filter is designed with 200 MHz bandwidth and central frequency 3.5 GHz . According to simulation results; the insertion loss s_{21} is -3.49 dB, return loss s_{11} is -16.94 dB at

3.5 GHz central frequency and -3 dB bandwidth is 199 MHz where upper and lower frequencies are 3617 MHz and 3418 MHz respectively. The stopband attenuation at 3.3 GHz is -33.33 dB and at 3.8 GHz is -50.81 dB. The designed filter is realized and measured; the insertion loss s_{21} is -3.23 dB, return loss s_{11} is -27.84 dB at 3.5 GHz central frequency and -3 dB bandwidth is 233 MHz where upper and lower frequencies are 3617 MHz and 3418 MHz respectively. The stopband attenuation at 3.3 GHz is -22.45 dB and at 3.8 GHz is -41.99 dB. The realized filter measurement and the designed filter simulation have similar results in filter response. The designed filter is realized and as a result low insertion loss, low cost of realization and high attenuation characteristic is achieved. If there are not any limitations at the designed filter application area dimensions, this realized filter has the advantage for low cost solutions.

Keywords: 1. Microstrip; 2. Bandpass Filter; 3. 5G NR Frequency Band; 4. Parallel Coupled

TABLE OF CONTENTS

JÜRİ VE ENSTİTÜ ONAYI	i
ŞEKİL ONAY SAYFASI.....	ii
ETİK İLKE VE KURALLARA UYUM BEYANI.....	iii
İNTİHAL RAPORU	Error! Bookmark not defined.
ACKNOWLEDGEMENTS	v
ÖZ	vi
ABSTRACT.....	viii
TABLE OF CONTENTS.....	x
LIST OF TABLES	xii
LIST OF FIGURES	xiii
ABBREVIATIONS	xvi
SYMBOLS.....	xviii
CURRICULUM VITAE.....	xx
SECTION 1. INTRODUCTION	1
1.1 Aim.....	3
1.2 Methodology	3
SECTION 2. LITERATURE REVIEW	5
2.1 Lumped and Distributed Elements in Filters	6
2.2 Filter Types	7
2.3 Low Pass Prototype Approach	8
2.4 Normalized Chebyshev Low-Pass Filter Prototype	10
2.5 Filter Transformation Types	13
2.5.1 Low-Pass Transformation	13
2.5.2 High-Pass Transformation.....	14
2.5.3 Band-Pass Transformation	15
2.6 Impedance and Admittance Inverters	16
2.6.1 Quarter-wave Length Transmission Line Invertors	17
2.7 Filter Realization with Transmission Line.....	18
2.7.1 Stripline	19
2.7.2 Coplanar Waveguide (CPW).....	20
2.7.3 Microstrip Line.....	21
2.8 Richard's Transformations.....	23
2.9 Kuroda's Identities.....	24
2.10 Resonator with Transmission Lines	27
2.10.1 Short-Circuited ($\lambda/4$) Length Transmission Line.....	27
2.10.2 Open-Circuited ($\lambda/2$) Length Transmission Line.....	28

2.11 Coupled Line Filters.....	30
2.11.1 Admittance Inverters and Coupling in Filter Design	33
2.11.2 Coupled Line Theory and Even-Odd-Mode Analysis.....	36
2.12 Calculation of Microstrip Dimensions	39
2.12.1 Akhtarzad’s Equations	39
2.12.2 Calculation of Parallel Coupled Line Filters Line Lengths.....	41
2.13 Input and Output of a Parallel Coupled Line Filter	42
2.13.1 Tapped Line Technique.....	43
SECTION 3. PARALLEL COUPLED MICROSTRIP BANDPASS FILTER DESIGN	45
3.1 Bandpass Filter Design	45
3.1.1 Chebyshev Low Pass Filter Prototype	45
3.1.2 Bandpass Transformation.....	47
3.1.3 Admittance Inverters and Even – Odd Mode Impedance Calculation.....	49
3.1.4 Parallel Coupled Microstrip Dimensions Calculation.....	51
3.1.5 Simulation of Parallel Coupled Microstrip Bandpass Filter	57
3.1.6 Measurement of Realized Design and Results.....	64
SECTION 4. CONCLUSION	67
REFERENCES	71

LIST OF TABLES

Table 2.1 Chebyshev low-pass prototype normalized element values passband ripple level 0.5 dB (Pozar, 2012)	10
Table 2.2 Chebyshev low-pass prototype normalized element values passband ripple level 3 dB (Pozar, 2012)	11
Table 2.3 Attributes comparison of stripline, CPW and microstrip line	22
Table 2.4 Coupled line circuits with various terminations (Pozar, 2012)	31
Table 3.1 Target filter specifications	45
Table 3.2 Chebyshev low pass filter prototypes element values for 0.5 dB ripple (Matthaei, Young, & Jones, 1980)	46
Table 3.3 Capacitor and inductor values of 5 th order bandpass filter	49
Table 3.4 Calculated parallel coupled line bandpass filter parameters.....	51
Table 3.5 Rogers RO4350 substrate specifications	52
Table 3.6 Calculated w/h dimensions of transmission lines	55
Table 3.7 Parallel coupled microstrip dimensions.....	57
Table 3.8 Even and odd mode impedance values comparassion	58
Table 3.9 Calculated dimensions of 3.5GHz bandpass filter.....	58
Table 3.10 Input and output 50 ohm line dimensions.....	58
Table 3.11 Designed filter dimensions	62
Table 3.12 Filter layout dimensions	63
Table 3.13 Simulated and realized filter response values.....	66
Table 4.1 Comparison of designed filters	69

LIST OF FIGURES

Figure 2.1 (a) Lumped elements resonators (b) Equivalent representation with distributed elements	6
Figure 2.2 Four types of the filter with attenuation versus angular frequency (Schaumann & Van Valkenburg, 2001).....	8
Figure 2.3 Response shapes of low pass (a) Butterworth filter (b) Chebyshev filter (c) Bessel filter (Floyd, 2012)	8
Figure 2.4 Low pass prototype filter with normalized elements (a) Pi network (b) T network (Hong & Lancaster, 2001)	9
Figure 2.5 Attenuation / normalized frequency, 0.5 dB ripple Chebyshev low pass filter prototype (Pozar, 2012).....	11
Figure 2.6 Attenuation / normalized frequency, 3 dB ripple Chebyshev low pass filter prototype (Pozar, 2012).....	12
Figure 2.7 Lowpass prototype to lowpass, highpass, bandpass and bandstop transformation (Pozar, 2012)	14
Figure 2.8 Shows impedance and admittance inverter (Pozar, 2012)	16
Figure 2.9 Impedance and admittance inverter (1) (Pozar, 2012)	16
Figure 2.10 Impedance and admittance inverter (2) (Pozar, 2012)	17
Figure 2.11 Impedance and admittance inverter (3) (Pozar, 2012)	17
Figure 2.12 Impedance matching $Z_0 = Z_{in}$ to Z_L (Edwards & Steer, 2016).....	18
Figure 2.13 Stripline (Edwards & Steer, 2016)	19
Figure 2.14 Electric and magnetic field lines of stripline (Pozar, 2012)	19
Figure 2.15 Coplanar wave-guide (Edwards & Steer, 2016).....	20
Figure 2.16 Coplanar waveguide geometry (Edwards & Steer, 2016).....	20
Figure 2.17 Microstrip transmission line (Edwards & Steer, 2016).....	21
Figure 2.18 Coupled microstrip line (Hong & Lancaster, 2001).....	22
Figure 2.19 Quarter-wave coupled and end coupled microstrip lines (Edwards & Steer, 2016)	22
Figure 2.20 (a) Richards transformation for an inductor, (b) for a capacitor (Pozar, 2012)	24

Figure 2.21 Kurado identities (Poazar, 2012).....	25
Figure 2.22 Kuroda identity (a) equivalent circuit (Poazar, 2012).....	25
Figure 2.23 Kuroda identity (b) equivalent circuit	26
Figure 2.24 (a) Low pass filter with inductors and capacitor, (b) Richard's Transformations applied form (Poazar, 2012) (edited by author)	26
Figure 2.25 Low pass filter 2 nd Kuroda identities is applied (Poazar, 2012) (edited by author)	27
Figure 2.26 Short-circuited $\lambda/4$ length lossy transmission line (Poazar, 2012).....	27
Figure 2.27 Open-circuited $\lambda/2$ length lossy transmission line (Poazar, 2012).....	29
Figure 2.28 Coupled open circuits (Poazar, 2012)	32
Figure 2.29 Bandpass network image impedance real part	33
Figure 2.30 Coupled transmission lines (Poazar, 2012).....	34
Figure 2.31 Equivalent of the coupled lines in Figure 2.30 (Poazar, 2012).....	34
Figure 2.32 n th order parallel coupled line filter (Poazar, 2012)	34
Figure 2.33 Equivalent capacitance network of three-wire lines (Poazar, 2012).....	36
Figure 2.34 Quasi-TEM modes of coupled lines; (a) Even mode excitation (b) Odd mode excitation (Hong & Lancaster, 2001).....	37
Figure 2.35 Even and odd mode characteristic impedance for symmetric coupled microstrip line on a substrate with $\epsilon_r = 10$ (Poazar, 2012)	38
Figure 2.36 Cross-sectional view (Hong & Lancaster, 2001)	39
Figure 2.37 Simple display of parallel coupled line filter	41
Figure 2.38 Microstrip open circuit and gap layout with electric fields (Edwards & Steer, 2016)	41
Figure 2.39 Parallel coupled line filter with equivalent effective length.....	41
Figure 2.40 (a) Standart 5 th order parallel coupled bandpass filter, (b) tapped input/output	44
Figure 3.1 Attenuation / normalized frequency; 0.5 dB ripple Chebyshev low pass filter prototype (Poazar, 2012).....	46
Figure 3.2 5 th order low pass prototype circuit	47
Figure 3.3 Low pass prototype to bandpass transformation	47
Figure 3.4 5 th order bandpass filter with lumped elements.....	49

Figure 3.5 Bandpass prototype filter with admittance inverters: (a) shunt resonators (b) series resonators	49
Figure 3.6 iFilter wizard even and mode values output for the desired filter.....	58
Figure 3.7 Filter layout	59
Figure 3.8 Bandpass filter EM simulation response	59
Figure 3.9 Bandpass filter EM simulation response with 3.5GHz central frequency	60
Figure 3.10 Bandpass filter optimization response IL and RL	60
Figure 3.11 Circuit diagram of the designed bandpass filter.....	61
Figure 3.12 Bandpass filter response with 3.5 GHz central frequency.	62
Figure 3.13 Microstrip filter layout.	62
Figure 3.14 Filter response with shifted central frequency	63
Figure 3.15 Microstrip filter new layout.....	64
Figure 3.16 Measurement of realized filter with network analyzer.....	64
Figure 3.17 Realized filter response measurement of first design.....	65
Figure 3.18 Parallel coupled microstrip bandpass filter	65
Figure 3.19 Realized filter response	66

ABBREVIATIONS

5G	: Fifth Generation
AWR	: Applied Wave Research
CPW	: Coplanar Waveguide
dB	: Decibel
EM	: Electromagnetic
Eq.	: Equation
GHz	: Giga hertz
GSM	: Global System for Mobile Communication
IL	: Insertion Loss
ISM	: Industrial, Scientific and Medical
L	: Length
LC	: Inductor Capacitor
LPP	: Low Pass Prototype
LTE	: Long-Term Evolution
MHz	: Megahertz
NR	: New Radio
oz	: Ounce
PCB	: Printed Circuit Board

RF : Radio Frequency
RL : Return Loss
S : Space
SMA : SubMiniature version A
TEM : Transverse Electro-Magnetic
W : Width
WLAN : Wireless Local Area Network



SYMBOLS

λ	: Wavelength
ϵ	: Dielectric Constant
f	: Frequency
v_p	: Velocity of Propagation
Ω	: Ohm
R	: Resistor
ω	: Angular Frequency
L	: Inductance
C	: Capacitance
Δ	: Fractional Bandwidth
K	: Impedance Inverter
J	: Admittance Inverter
Z	: Impedance
β	: Propagation Constant
X	: Reactance
θ	: Angle in Radians
α	: Attenuation
π	: pi

l_{eo} : Equivalent Effective Length

Q_{SL} : Singly Loaded Quality Factor



CURRICULUM VITAE

İsmail Oğuz Saylan

Department of Electrics-Electronics Engineering

Education

B. Sc. 2009 Yeditepe University, Department of Electrical and
Electronics Engineering
High School 2004 Rahmi Kula Anatolian High School

Work Experience

2012-present Software Test Engineer – Huawei Technologies
2009-2010 Sales Engineer - Makelsan Machine Chemistry Electronic Industry
& Trade
2008 Intern - İşbir Electric San. A.Ş.

Personal Information

Data of Birth : Balıkesir, 1986 Gender: M
Language Skills : English (Advance)
GSM / e-mail : 05336334268 / iosaylan@gmail.com

SECTION 1. INTRODUCTION

In the near future, GSM operators will start using the emerging Fifth Generation (5G) technology to allow data exchange at higher speeds as well as many advantages. According to such new technology, new frequency bands are proposed. The New Radio (NR) 5G technology carries the frequency bands used for communication above 3 GHz (URL-1, 2018).

The NR 5G n78 (3.3 GHz to 3.8 GHz) band is planned to be used mostly by Europe, China and Australia (Shin & Eilert, 2018). Some European countries define frequency bands for GSM operators in the n78 band. One of the European countries which is started to work in the n78 band of NR 5G is the United Kingdom. Frequencies which will be used by UK GSM operators is between 3.4 GHz to 3.6 GHz. According to global groups, particular interest to the n78 band, more base stations, cell phones, and communication devices are expected to support the n78 band near future (URL-2, 2018).

New bandpass filter designs play an important role to avoid interference by suppressing of adjacent bands whose spectrums are expected to increase in NR 5G technology. One of them is NR 5G n41 band (2.5 GHz to 2.7 GHz) which is used currently for the traditional industrial, scientific and medical purposes named as ISM band. The ISM band which is a commonly accepted at 2.54 GHz frequency for worldwide operations (Shin & Eilert, 2018). The upper adjacent is (4.9 GHz to 5.0 GHz) which is used as a WLAN band to expand band spectrum to lower frequency to support more channels. Depending on the intensity of use in adjacent bands in the near future, a bandpass filter designed for the n78 band requires good attenuation at 2.7 GHz and 4.9 GHz. In (Shin & Eilert, 2018), the designed bandpass filter with 3.3 to 3.8 GHz passband which meets 5G n78 band demonstrated a size benefit with good insertion loss <1.8 dB and attenuations characteristic >30 dB at 2.7 GHz and 4.9 GHz to filter out adjacent bands.

There are different types of microstrip line filters; hairpin, step impedance and parallel coupled line. Some works about microstrip parallel coupled line filter design details will be given as examples. In (Al-Areqi, Seman, & Rahman, 2017), a parallel coupled line microstrip bandpass filter for the application 5G wireless communication was defined and optimized using Rogers RO4003C substrate with center frequencies of 5 GHz, 15 GHz and 28 GHz. The designed bandpass filter demonstrates an optimal average performance of 8.59% bandwidth with an insertion loss of 1.53 dB and return loss greater than 12 dB.

Another parallel coupled line bandpass filter proposed in (Seghier, Benahmed, Bendimerad, & Benabdallah, 2012) for frequency modulation (FM) application using

Rogers RO4003C substrate at 6 GHz bandwidth of 200 MHz and minimum attenuation of -15 dB at 6.2 GHz, passband ripple of 0.5 dB. It is designed using half wave long resonators and admittance inverters.

In addition to the works mentioned here, there are a lot of other works related to parallel coupled bandpass filters. Only some of them are picked and used as a reference to decide for bandpass filter specifications.

In this thesis, a parallel coupled line microstrip bandpass filter is designed at 3.5 GHz with 200 MHz for NR 5G n78 band applications using the RO4350 substrate with the help of AWR iFilter wizard software.

In the second chapter, literature is reviewed based on reviewed articles and books. The name of articles and main books used in literature are given. Firstly, articles on parallel coupled microstrip bandpass filter design are reviewed. According to the review of works, filter design sections are defined. Secondly, subjects of fundamental books that are related to filter design and defined by article reviews are summarized. The outlined topics are 'Lumped and Distributed Elements in Filters', 'Filter Types', 'Low Pass Prototype', 'Normalized Chebyshev Low-Pass Filter Prototype', 'Filter Transformation Types', 'Impedance and Admittance Inverters', 'Filter Realization with Transmission Line', 'Richard's Transformations', 'Kuroda's Identities', 'Resonator with Transmission Lines', 'Coupled Line Filters', 'Calculation of Microstrip Dimensions', 'Input and Output of a Parallel Coupled Line Filter' with a given sequence.

In the third chapter, according to the literature review and emerging technology trend, bandpass filter specifications are chosen to design a new filter for being used in new applications. And these specs are used to design a bandpass filter. The designed filter is simulated with the use of AWR software. For the realized filter; insertion loss, return loss, bandwidth and central frequency values are measured and these are compared with the simulation results.

In the last chapter, designed and realized parallel coupled bandpass filter measurement results are evaluated with AWR software simulation results. Using simulated filter dimensions, the parallel coupled microstrip bandpass filter is realized using RO4350 as a substrate. The desired response is achieved in the realized filter measurement in the laboratory using a network analyzer. Both designed and realized filter response results are similar. The realized filter has low insertion loss and high return loss at central frequency. The bandwidth of the filter is covers the n78 band 3400 Mhz to 3600 MHz frequency range. The stopband attenuations at the edge of the n78 frequency band are high enough to block interference from adjacent bands. The filter size can be acceptable due to the system design which the filter will be used with cheap realization cost.

1.1 Aim

One of the most important component used in communication systems is filters. A large number of filters used in the applications allows working properly of the devices operating at different and near frequencies. With the new technologies, the number of instruments used at the same frequency increases day by day. Filters are designed according to the application to be used in different types, sizes, and specifications. In order to keep wireless communication up to date numerous researches on component design being conducted including bandpass filter (Al-Areqi, Seman, & Rahman, 2017) (Mahon, 2017) (Albreem, 2015).

5G NR technology, which has been used to meet the evolving needs and will become very widespread in the near future, necessitated new filter designs. 5G NR technology has many frequency channels. The n78 channel has a range of 3300 to 3800 MHz, one of the frequency ranges used in 5g technology (Shin & Eilert, 2018) (URL-1, 2018). 5G NR frequencies bands were distributed to GSM operators for use in the UK. According to the results of the auctions, the frequency range of the current situation (3400 - 3600 MHz) was officially given to the use of GSM operators (URL-2, 2018).

The aim of the thesis is to design, to simulate and to realize of a 5th degree parallel coupled microstrip bandpass filter with a 3.5 GHz central frequency for to use 5G NR technology applications, 200 MHz bandwidth, high attenuation characteristics in the stopband, low insertion loss and low cost of realization.

1.2 Methodology

In the literature review chapter of the thesis, filter and filter related topics are examined. A research was conducted to determine the needs arising from current technology approaches. Current technology approaches are used to determine the central frequency and bandwidth of the filter to be designed.

Numerous frequencies have been defined for 5G NR technology, which will be used more in the near future. One of the frequencies defined is the 3.5 GHz (3300-3800) n78 band. For the 5G NR n78 band, it was decided to design a filter with high attenuation characteristics in the stopband regions, stable in the passband area and low insertion loss in order to prevent interference caused by adjacent bands. The bandwidth of the n78 band (3.3 - 3.8 GHz) is 500 Mhz. In the current situation, the frequency range planned to be used in the UK is the range of 3.4 - 3.6 GHz having a bandwidth of 200 MHz (URL-1, 2018) (URL-2,2018).

Generally, in bandpass filter design parallel coupled inductor and capacitor are used to resonate at desired frequency and shunt resonators are grounded to attenuate the frequencies outside of the passband. The series inductor and capacitor couples are also

used to pass desired frequencies. Beside on given specification, microstrip transmission lines should be used rather than lumped elements due to high frequency. According to the restriction about a lumped element, a parallel coupled microstrip is used to design a bandpass filter.

The filter design was started by selecting the low-pass filter type. Butterworth, Chebyshev and Bessel filters responses were examined. Although Chebyshev has ripple in the passband region, it has better stopband attenuation than other filter types, therefore, Chebyshev 0.5 dB ripple in the passband filter was decided to use in the design. To suppress the interference caused by adjacent bands as stopband attenuation > -40 dB at 3.8 GHz, the filter degree was calculated as the fifth order.

A 5-degree low pass prototype filter was designed using Chebyshev circuit element values.

The designed low pass prototype filter was transformed to a lumped element bandpass filter and element values were calculated with transformation equations. To transform the lumped element filter circuit to parallel coupled line filter, admittance invertors were inserted between the shunt resonators. The values of the admittance invertors were calculated. With the results of them, even and odd mode impedance of parallel couples were calculated.

For the simulation and realization, RO4350 PCB substrate was decided to use. Equations for the calculation of physical dimensions required for the design are shown and according to given equations, the width (w) and space (s) of parallel coupled lines were calculated with the use of even and odd mode impedance values. For the calculation of the length (l) of parallel coupled lines were used effective dielectric constant values. The width (w), and length (l) of resonators and space (s) between parallel coupled lines values were also figured out with the AWR iFilter simulation software.

The simulation of the filter was performed with the AWR iFilter software and for the realization, the filter was realized on the chosen material RO4350. The measurements of the realized filter were made at laboratory using a network analyzer. The results of the laboratory measurements were compared with the simulation results.

SECTION 2. LITERATURE REVIEW

In this chapter, topics are focused on the theory of filter design and realization of a microstrip parallel coupled line bandpass filter. Firstly, literature related to new technologies and works to support new technologies are reviewed and the result of this review is shared in the introduction section of the first chapter. After the thesis subject was determined, similar articles about this subject were examined and the topics that will guide the filter design in the thesis were defined and the method of the thesis work was formed. Topics are related to bandpass filter design but also for other response types some substantial subjects are evaluated in this chapter by showing fundamental references. Sample figures are given to make the topic more comprehensible. The sequence of sections is given in an order similar to the design process.

Among the works examined on the subject, highlighted articles are the following:

- In this “Parallel Coupled Microstrip Bandpass Filter Designed and Modeled at 2 GHz” named article, author (Vipul M Dabhi) shows the design technique, parametric analysis, and simulated and realized results of parallel coupled transmission line filter and gives design equations for calculation of coupled line parameters space gap between lines, line widths and lengths are and define the theoretical design process of the filter (Vipul & Ved, 2016).
- This “Parallel-Coupled Line Bandpass Filter Design Using Different Substrates for Fifth Generation Wireless Communication Applications” named article author (Nadera Najib Al-Areqi) used quarter wave parallel-coupled line resonators and additional small resonator attached between the first/last coupled-line section and the ports’ 50 ohm transmission line to design filter. And the effect of a substrate in the bandwidth performance is examined (Nadera, Norhudah, & Tharek, 2015).
- In this “Improved Design Equations of the Tapped-Line Structure for Coupled-Line Filters” named article, coupled-line filters with tapped input and output are worked by the author (Chih-Ming Tsai) (Tsai, 2007).
- The author is in “Development of 5.8 GHz Microstrip Parallel Coupled Line Bandpass Filter for Wireless Communication System” article show the design technique, parameter analysis, real prototype realization, and measurement results compare to simulation (Othman, Sinnappa, Hussain, Aziz, & Ismail, 2013).
- In this article, “Design and Simulation of a Parallel-Coupled Microstrip Bandpass Filter” author has examined the calculation of even-mode and

odd-mode characteristic impedances of coupled line pairs (Yang, Cross, & Drake, 2014).

- This “The Complete Design of Microstrip Directional Couplers Using the Synthesis Technique” named article author (Abdullah Eroglu) examined a symmetrical technique to design microstrip directional coupler (Eroglu & Lee, 2008).

Main books which are used to outline sections are; “Microwave Engineering 4th Edition” by David M Pozar, “Foundations for Microstrip Circuit Design” by Terry C. Edwards, Michael B. Steer, “Microstrip Filters for RF Microwave Applications” Jie Sheng Hong, M. J. Lancaster, “RF and Microwave Coupled Line Circuits Second Ed” R. K. Mongia, I. J. Bahl, P. Bhartia, J. Hong, “RF Circuit Design Theory and Applications” Reinhold Ludwig, Pavel Bretchko, “Design of Analog Filters” Rolf Schaumann, Mac E. Van Valkenburg are selected as main reference books.

2.1 Lumped and Distributed Elements in Filters

Lumped elements are resistor, inductor or capacitor. A distributed element is a specifically defined part of the transmission line. A distributed element can be realized with a cavity in a waveguide, coaxial cable or copper on a board. Figure 2.1 shows lumped elements resonators with capacitance and inductances and equivalents representation with distributed elements. (Edwards & Steer, 2016)

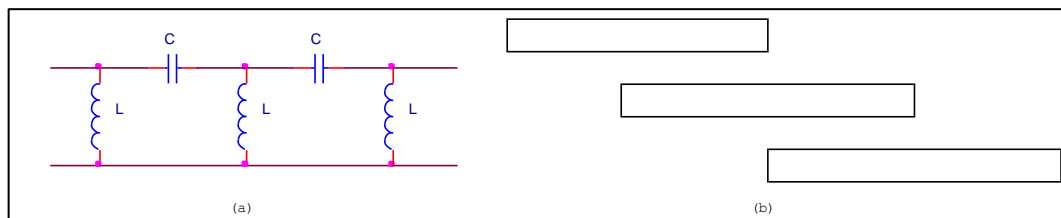


Figure 2.1 (a) Lumped elements resonators (b) Equivalent representation with distributed elements

In practice, distributed elements are useful in high frequency and lumped elements in low frequencies. The relationship between frequency and wavelength means that as frequencies increase, lumped elements become unreliable as the length of the components approaches the 0.1th guideline with respect to wavelength (Pozar, 2012).

The wavelength (λ) is calculated by the velocity of propagation (v_p) and the highest frequency (f) of the operation. Transmission lines have importance in high frequency applications (Pozar, 2012).

$$\lambda_{eff} = \frac{V_p}{f} \quad (2.1)$$

Distributed element is a part of transmission line inductive or capacitive elements can be realized simply. In the later section, lumped and distributed components are used to make filter design. As a starting point, lumped elements are used and then transformation is applied to create the equivalent of this circuit with distributed elements to use the filter in microwave frequencies (Edwards & Steer, 2016) (Levy, Snyder, & Matthaei, 2002).

2.2 Filter Types

Filters are basically classified according to passing and attenuating frequencies. According to the frequency range, there are four main types of filters. These are low-pass, high-pass, band-pass and band-stop. In an ideal filter, signals passing through passbands are not attenuated and gained. However, in such an ideal type filter, stopband signals are completely blocked (Schaumann & Van Valkenburg, 2001).

Low pass filters pass all frequencies till cut off frequency starting from zero. High pass filters pass all frequencies above cut off frequency till infinity. Bandpass filter passes signals between two specified frequency ranges and attenuates all signals out of this range. Band stop filter attenuates all signals between two specified frequency ranges and passes all signals out of this range (Mongia, Bahl, Bhartia, & Hong, 2007) (Schaumann & Van Valkenburg, 2001) (Edwards & Steer, 2016) (Hinton, 1980) (Abbas, Zubair, & Mojeeb).

The filters can be also classified according to filter response shapes. Mostly used low pass prototype ones are Butterworth filter, Chebyshev filter and Bessel filter (Figure 2.2) (Schaumann & Van Valkenburg, 2001).

Butterworth filter is also known as a maximally flat filter. Response shape is maximally flat in the passband and there is no ripple, steep transition from pass band to stop band. Chebyshev filters are also called as equal ripple filters. The response has ripples in the passband region and has a steeper transition from pass band to stop band. Bessel filters are also known as maximally flat time delay filters. Response shape has a relatively gentle transition from pass band to stop band and a uniform phase delay in passband region (Figure 2.3) (Çakır, Gündüz, & Sevgi, 2006).

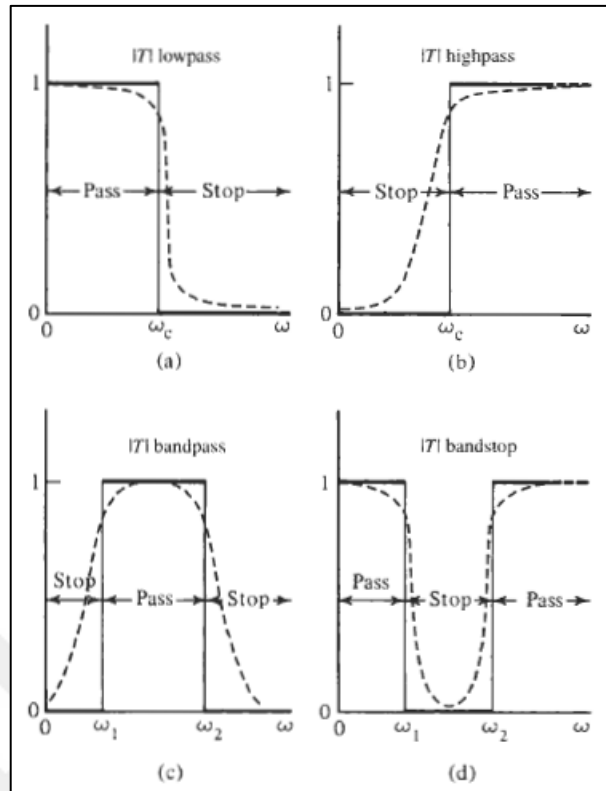


Figure 2.2 Four types of the filter with attenuation versus angular frequency (Schaumann & Van Valkenburg, 2001)

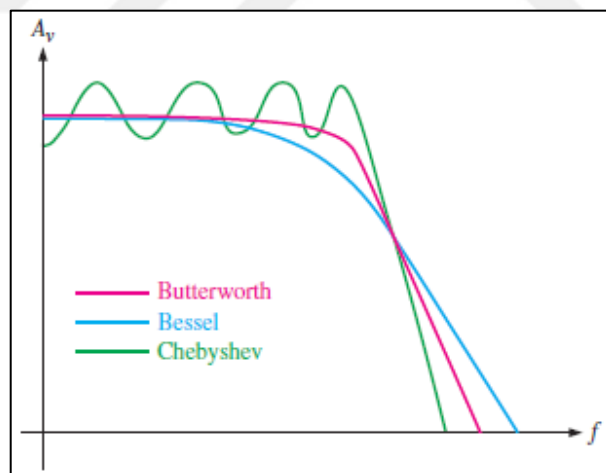


Figure 2.3 Response shapes of low pass (a) Butterworth filter (b) Chebyshev filter (c) Bessel filter (Floyd, 2012)

2.3 Low Pass Prototype Approach

Matthaei, Young, and Jones popularized the low pass prototype approach, which is very useful for filter design (Matthaei, Young, & Jones, 1980). A low pass prototype can be used as a starting point of filter design. In this prototype, normalized impedance and frequency are defined. Transformation is needed to get the desired frequency range

and impedance. Low pass prototype which response shapes commonly used in Butterworth, Chebyshev, and Bessel filters (Ludwig & Bretchko, 2000).

The elements of low pass filter prototype are numbered from g_0 at the generator side to g_{n+1} at the load side. The elements are changed according to network topology. These topologies are Pi network and T network. There is not any difference at the performance whether Pi network or T network topology is used because both are dual from each other. However, it affects the types of distributed resonators, which could be used later in filter design (Ludwig & Bretchko, 2000).

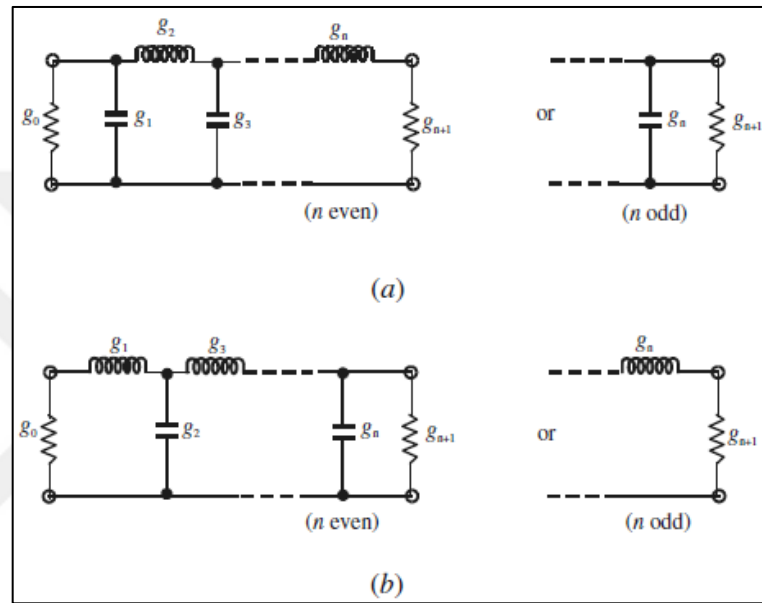


Figure 2.4 Low pass prototype filter with normalized elements (a) Pi network (b) T network (Hong & Lancaster, 2001)

The elements ‘g’ are defined as below:

$$g_0 = \begin{pmatrix} \text{resistance for generator Pi network} \\ \text{conductance for generator T network} \end{pmatrix}$$

$$g_{(1 \text{ to } N)} = \begin{pmatrix} \text{inductance for series inductance} \\ \text{capacitance for shunt capacitor} \end{pmatrix}$$

$$g_{(N+1)} = \begin{pmatrix} \text{resistance for load if } g_n \text{ is a shunt capacitor} \\ \text{conductance for load if } g_n \text{ is a series inductor} \end{pmatrix}$$

g_0 can be resistance or conductance according to the network topology,

$g_{(1 \text{ to } N)}$ alternates between inductance (series inductance) and capacitance (shunt capacitor),

$g_{(N+1)}$ can be load resistance or conductance according to the number of circuit elements (Ludwig & Bretchko, 2000).

2.4 Normalized Chebyshev Low-Pass Filter Prototype

As previously discussed, the low-pass prototype approach which is simplified by Matthaei, Young and Jones, can be applied to specific response shape filters. The element values "g" can be calculated using the network synthesis method developed by Brune and Darlington (Schaumann & Van Valkenburg, 2001). Previously calculated element values are given in tables, which are available for different response shapes such as Butterworth and Chebyshev which can be found in the literature (Matthaei, Young, & Jones, 1980)(Pojar, 2012). These tables include normalized element values as assuming $\omega' = 1 \text{ rad / sec}$ and $g_o = 1$. In filter prototypes, a number of reactive elements is equal to the order of filter (Pojar, 2012) (Ludwig & Bretchko, 2000). In most cases, the sharper transition is desired between pass-band and stop-band. It can be achieved by increasing the number of circuit elements (order of filter) (Schaumann & Van Valkenburg, 2001).

Table 2.1 Chebyshev low-pass prototype normalized element values passband ripple level 0.5 dB (Pojar, 2012)

N	0.5 dB Ripple										
	g_1	g_2	g_3	g_4	g_5	g_6	g_7	g_8	g_9	g_{10}	g_{11}
1	0.6986	1.0000									
2	1.4029	0.7071	1.9841								
3	1.5963	1.0967	1.5963	1.0000							
4	1.6703	1.1926	2.3661	0.8419	1.9841						
5	1.7058	1.2296	2.5408	1.2296	1.7058	1.0000					
6	1.7254	1.2479	2.6064	1.3137	2.4758	0.8696	1.9841				
7	1.7372	1.2583	2.6381	1.3444	2.6381	1.2583	1.7372	1.0000			
8	1.7451	1.2647	2.6564	1.3590	2.6964	1.3389	2.5093	0.8796	1.9841		
9	1.7504	1.2690	2.6678	1.3673	2.7239	1.3673	2.6678	1.2690	1.7504	1.0000	
10	1.7543	1.2721	2.6754	1.3725	2.7392	1.3806	2.7231	1.3485	2.5239	0.8842	1.9841

Table 2.2 Chebyshev low-pass prototype normalized element values passband ripple level 3 dB (Pozar, 2012)

3.0 dB Ripple											
N	g_1	g_2	g_3	g_4	g_5	g_6	g_7	g_8	g_9	g_{10}	g_{11}
1	1.9953	1.0000									
2	3.1013	0.5339	5.8095								
3	3.3487	0.7117	3.3487	1.0000							
4	3.4389	0.7483	4.3471	0.5920	5.8095						
5	3.4817	0.7618	4.5381	0.7618	3.4817	1.0000					
6	3.5045	0.7685	4.6061	0.7929	4.4641	0.6033	5.8095				
7	3.5182	0.7723	4.6386	0.8039	4.6386	0.7723	3.5182	1.0000			
8	3.5277	0.7745	4.6575	0.8089	4.6990	0.8018	4.4990	0.6073	5.8095		
9	3.5340	0.7760	4.6692	0.8118	4.7272	0.8118	4.6692	0.7760	3.5340	1.0000	
10	3.5384	0.7771	4.6768	0.8136	4.7425	0.8164	4.7260	0.8051	4.5142	0.6091	5.8095

Chebyshev low-pass prototype filter normalized element values are given in Table 2.1 and Table 2.2. In Table 2.1, element values exist for designing Chebyshev low-pass prototype filter with a normalized source impedance ($g_0' = 1$), cut-off frequency ($\omega_c' = 1$ rad/s) and passband ripple level 0.5 dB or in Table 2.2 same values exist for passband ripple level 3 dB. These element values can be used both π and T network type filter topologies. The element values can be inductance value or capacitor value according to selected topologies.

The filter order can be decided using previously define attenuation responses for low pass prototype filters. Attenuation versus normalized frequency for a Chebyshev filter prototype is given in Figure 2.5 passband ripple is 0.5 dB and in Figure 2.6 passband level 3 dB ripple.

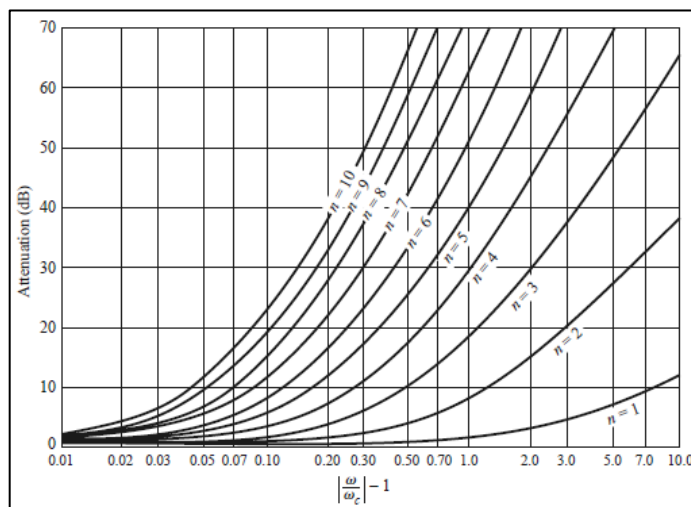


Figure 2.5 Attenuation / normalized frequency, 0.5 dB ripple Chebyshev low pass filter prototype (Pozar, 2012)

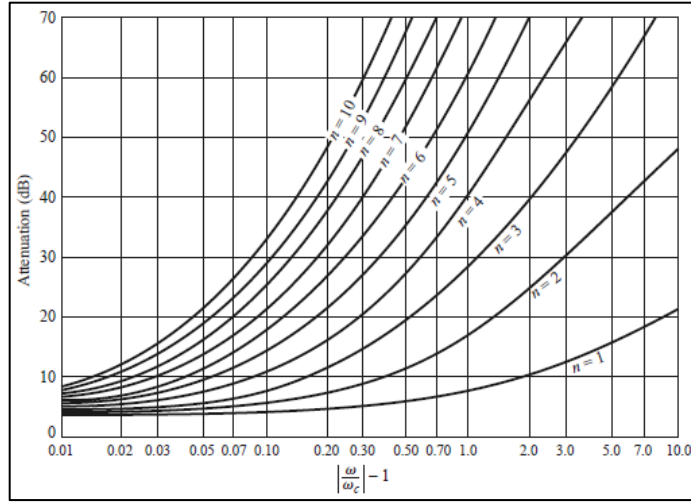


Figure 2.6 Attenuation / normalized frequency, 3 dB ripple Chebyshev low pass filter prototype (Pozar, 2012)

According to design specification, if the value of wanted attenuation is known, the order of filter can be decided using these attenuations versus normalized frequency figures. The equation for calculation of filter order is given below (Hong & Lancaster, 2001).

$$f_0 = \sqrt{f_1 \cdot f_2} \quad (2.2)$$

$$FBW = \frac{f_2 - f_1}{f_0} \quad (2.3)$$

$$f_n = \frac{1}{FBW} \cdot \left(\frac{f_1}{f_c} - \frac{f_c}{f_1} \right) \quad (2.4)$$

Normalized frequency; $\left| \frac{f_n}{1} \right| - 1 \quad (2.5)$

According to normalized frequency calculated using attenuation graphs order of filter can be decided. Generator and load element values are equal to each other when the order of the filter is odd. In design using Chebyshev filter prototype, load element values are alternating according to the number of N if N is odd it equals 1 and in even condition, it creates a mismatch between the generator and load impedance. Quarter wave transformer or adding new filter element is a solution for making N odd (Pozar, 2012).

2.5 Filter Transformation Types

In the filter transformation, the low pass prototype filter which has normalized source impedance of $R_s=1 \Omega$, a cutoff frequency of $\omega_c = 1$ rad/s and normalized element values are used as a starting design. To transform a low pass prototype filter, both impedance and frequency scaling is needed. Impedance scaling is applied to component values L , C and R_L of original prototype, equations are given below. R_o is equal to desired filter source resistance hence source resistance of prototype filter is an equal one. In the below scaled impedance values of filter components equations are given (Pojar, 2012) (Matthaei, Young, & Jones, 1980).

$$L' = R_o L \quad (2.6)$$

$$C' = \frac{C}{R_o} \quad (2.7)$$

$$R_s' = R_o \quad (2.8)$$

$$R_L' = R_o R_L \quad (2.9)$$

The cutoff frequency of a low pass prototype is equal to one as $\omega_c = 1$, to scale the frequency replacing ω by ω/ω_c is applied. In this case, new cutoff frequency occurs when $\omega/\omega_c = 1$ or $\omega = \omega_c$ (Pojar, 2012) (Matthaei, Young, & Jones, 1980).

2.5.1 Low-Pass Transformation

At the transformation of low-pass prototype filter to a low-pass filter, inductors and capacitors both are remains as inductors or capacitors. The calculation equations to make load impedance 50Ω are given below (Hong & Lancaster, 2001) (Collin, 2001) (Pojar, 2012).

$$\begin{aligned} R_s' &= R_s \cdot R_o \\ R_s' &= 1 \cdot 50ohm = 50\Omega \end{aligned} \quad (2.10)$$

$$\begin{aligned} R_L' &= R_L \cdot R_o \\ R_L' &= 1 \cdot 50ohm = 50\Omega \end{aligned} \quad (2.11)$$

The value of resistance is frequency independent so it can be scaled to any value directly by multiplying element values with scaled value in case of N is odd. The circuit

normalized elements remain as same with low pass prototype in low pass filter. To provide filtering at the desired value, frequency scaling is needed for normalized element values of g_1 to g_N .

As previously discussed, these elements can be capacitors or inductors according to design topology. As an example, in π network g_1 is used as shunt capacitor. The calculation for these element values for the desired frequency is given below.

$$\omega = 2\pi f \quad (2.12)$$

$$L'_k = \frac{R_0 \cdot g'_k}{\omega_c} \quad (2.13)$$

$$C'_k = \frac{g'_k}{R_0 \cdot \omega_c} \quad (2.14)$$

Using low-pass prototype, other types of filter also can be derived using a transformation impedance scale and normalized element scales at a specific frequency. In Figure 2.7, lowpass prototype to lowpass, highpass, bandpass and bandstop transformations are shown. The equations in Figure 2.7 does not include impedance scaling (Collin, 2001).

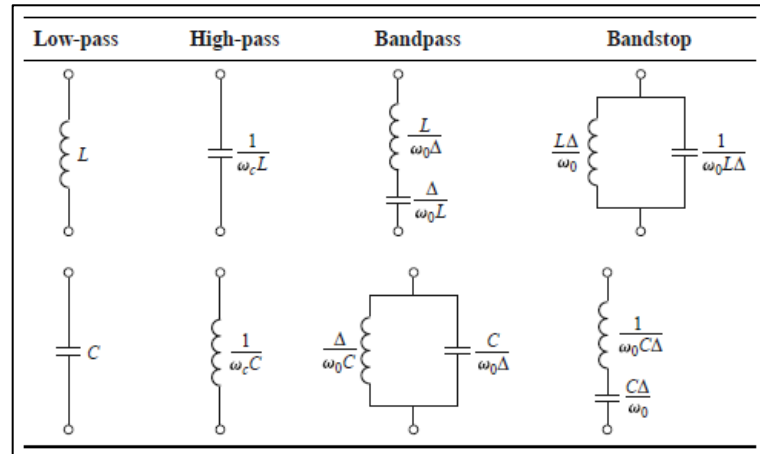


Figure 2.7 Lowpass prototype to lowpass, highpass, bandpass and bandstop transformation (Pozar, 2012)

2.5.2 High-Pass Transformation

At the transformation of low-pass prototype filter to a high-pass filter, inductors are replaced with a capacitor and capacitor with an inductor. Using normalized element

values in low-pass prototype, translated values of elements can be calculated with below equations for the high-pass filter (Collin, 2001).

$$C_n = \frac{1}{\omega_c \cdot g_n \cdot R_o} \quad (2.15)$$

$$L_n = \frac{R_o}{\omega_c \cdot g_n} \quad (2.16)$$

2.5.3 Band-Pass Transformation

At the transformation of low-pass prototype filter to band-pass filter, inductors are changed with series inductor and capacitor, capacitances are changed with parallel inductor and capacitor which are shown in Figure 2.7.

Band-pass transformation is slightly different from low-pass and high-pass transformation because pass-band is defined between two specific frequencies denoted as ω_1 and ω_2 (Pozar, 2012). The center frequency ω_0 can be calculated as the arithmetic mean of ω_1 and ω_2 ; but to make it simpler, geometric mean is used.

Using fractional bandwidth and central frequency in transformation equations, normalized elements values can be scaled according to design specifications. The central frequency and fractional bandwidths can be calculated with the below equations.

$$\omega_0 = \sqrt{\omega_1 \cdot \omega_2} \quad (2.17)$$

Fractional bandwidth of pass-band is;

$$\Delta = \frac{\omega_2 - \omega_1}{\omega_0} \quad (2.18)$$

By using these two values, element values can be calculated for a band-pass filter with below equations:

For inductor to series inductor and capacitor;

$$L_n = \frac{g_n \cdot R_o}{\omega_0 \cdot \Delta} \quad (2.19)$$

$$C_n = \frac{\Delta}{\omega_0 \cdot g_n \cdot Z_o} \quad (2.20)$$

For capacitor to parallel inductor and capacitor;

$$L_{in} = \frac{\Delta \cdot R_0}{\omega_0 \cdot g_n} \quad (2.21)$$

$$C_n = \frac{g_n}{\omega_0 \cdot \Delta \cdot Z_0} \quad (2.22)$$

2.6 Impedance and Admittance Inverters

Designing with using the same type of elements helps to filter calculation. Karado identities can be used for this purpose to change series elements. Series elements can be changed with shunt ones or vice versa. Another method to change elements connections in the circuit is to utilize impedance (K) or admittance (J) inverters according to the desired design (Edwards & Steer, 2016). This (K) impedance or (J) admittance inverters in Figure 2.8 can be realized using the below options (Pozar, 2012) (Seghier, Benahmed, & Benabdallah).

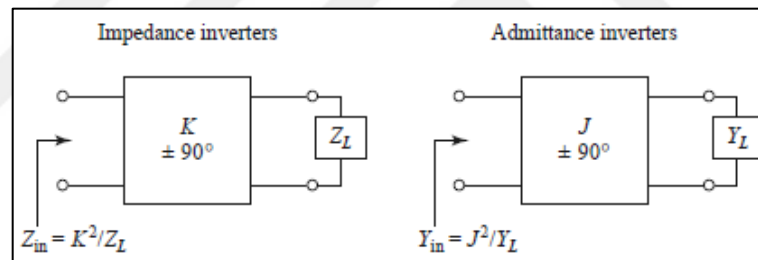


Figure 2.8 Shows impedance and admittance inverter (Pozar, 2012)

- 1) A quarter-wave transformer.

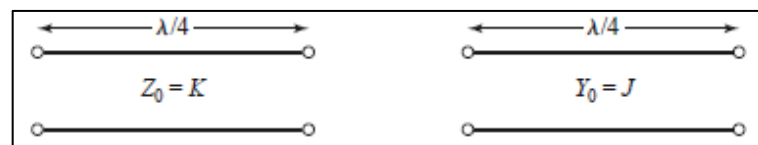


Figure 2.9 Impedance and admittance inverter (1) (Pozar, 2012)

2) Transmission lines and reactive elements.

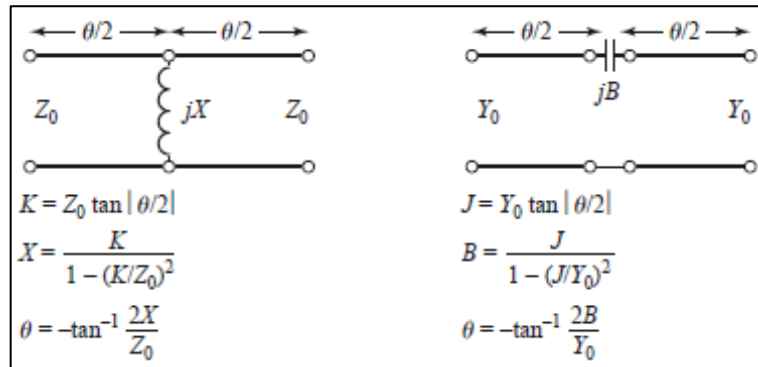


Figure 2.10 Impedance and admittance inverter (2) (Pozar, 2012)

3) Capacitor networks.

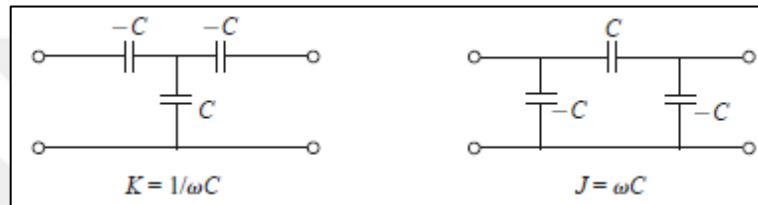


Figure 2.11 Impedance and admittance inverter (3) (Pozar, 2012)

Realization technique and type of filter which will be designed take a role when inverter type is chosen. In some cases, one type has an advantage over another. Impedance inverters show load impedance Z_L as an inverse to the rest of circuit Z_{in} with an element which characteristic impedance is K shown in Figure 2.8. Similarly, admittance inverter show load admittance Y_L as an inverse to rest of circuit Y_{in} using a unit element with admittance J (Seghier, Benahmed, & Benabdallah) (Hong & Lancaster, 2001) (Ferh & Jleed).

2.6.1 Quarter-wave Length Transmission Line Invertors

A simple way to implement an impedance inverter is to use a $\lambda/4$ length of the transmission line. Quarter-wave length ($\lambda/4$) of transmission line behaves like an inverter, and this nature is can be described with sin wave. In the sin wave oscillation amplitude changes from zero to the maximum amplitude at each $\lambda/4$ length.

This nature of quarter-wave ($\lambda/4$) transmission line makes it useful as an inverter. In below Figure 2.12 Z_L load impedance matches to Z_{in} which equals to Z_0 .

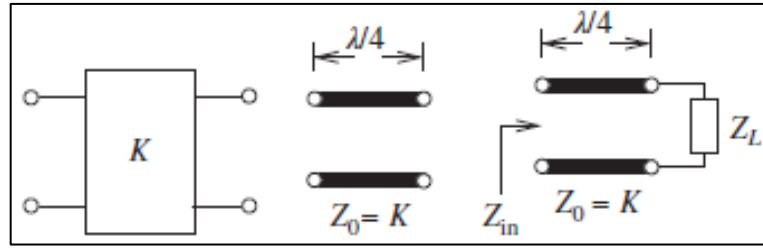


Figure 2.12 Impedance matching $Z_0 = Z_{in}$ to Z_L (Edwards & Steer, 2016)

To calculate Z_0 :

$$Z_{in} = \frac{Z_0^2}{Z_L} \quad (2.23)$$

With using a $\lambda/4$ inverter with Z_0 impedance, the condition $Z_0 = Z_{in}$ impedance match is achieved. In this example, impedance inverter K makes the load impedance Z_L appear like a characteristic impedance Z_0 to the rest of the circuit Z_{in} . The same procedure can be used to apply admittance inverters (Edwards & Steer, 2016) (Collin, 2001).

2.7 Filter Realization with Transmission Line

There are several alternative types of transmission lines exist to construct distributed elements. Type of transmission line technologies which is used to realize filter design should be selected before transmission lines transformation is applied.

Coaxial lines, waveguides and planar transmission lines can be utilized as media or transmission lines. When considering bandwidth, the coaxial line is convenient for test applications with very high bandwidth. Waveguides are big in size and expensive despite its high power handling capability and low loss (Pozar, 2012).

Stripline, microstrip, slotline, coplanar waveguide and other types of related geometries is composed with planar transmission lines. Planar transmission lines are alternative to retire devices such as diodes and transistors for microwave integrated circuits with compact, low cost and easy integration features. With thin substrates, the frequency dependence of the line is decreased in microstrip lines. This makes microstrip is mostly preferred media for microwave filter applications. In the following sections, some of planar transmission line media will be discussed (Pozar, 2012) (Wadell, 1991).

2.7.1 Stripline

A planar type of transmission line that consists of three layers, a signal conductor in the middle of two ground planes. Stripline transmission lines geometry is shown in Figure 2.13.

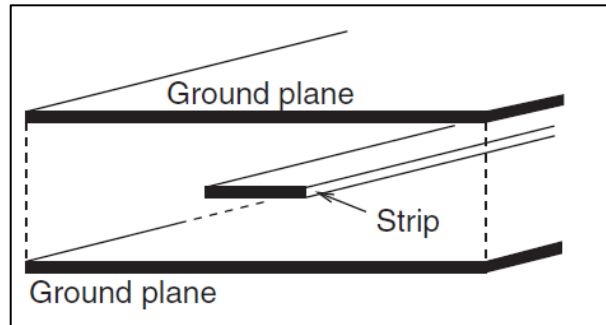


Figure 2.13 Stripline (Edwards & Steer, 2016)

Between ground planes and signal conductors in the middle is a field with a uniform dielectric material, dielectric constant ϵ . This self-shielded geometry gives some advantages to the stripline transmission line. Figure 2.14 shows the electrical and magnetic field lines in stripline geometry. Self-shielded structure decreases radiation loss in this type of transmission line and behaves electrically stable (Edwards & Steer, 2016).

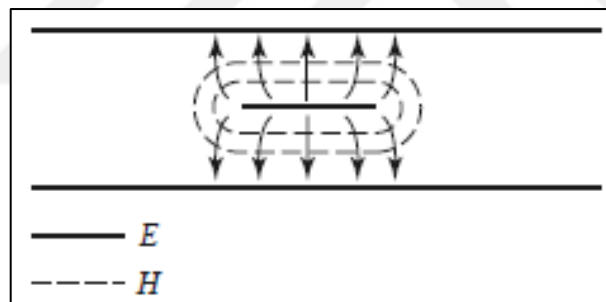


Figure 2.14 Electric and magnetic field lines of stripline (Pozar, 2012)

The characteristic impedance is controlled by the signal conductor width, the distance ground planes do not affect characteristic impedance. And also this type of transmission line has some disadvantages according to other types. Realization of the stripline transmission lines is difficult. This structure cannot be constructed with traditional PCB realization techniques because geometry includes a number of layers. Access to signal conductor is difficult because it is encapsulated between two dielectric layers. The difficulties and complexity in the realization technique increase the cost. Considering, for microwave circuit adding other components to stripline can be a problem because of to access the signal conductor (Pozar, 2012) (Edwards & Steer, 2016) (Wadell, 1991).

2.7.2 Coplanar Waveguide (CPW)

The coplanar waveguide has one signal carrying conductor on a top layer and ground planes that are located on the top layer as the signal conductor. CPW was invented in 1969 by C.P. Wen (WEN, 1969). Below top layer uniform dielectric material where the dielectric constant ϵ exists, and the surrounding material for a signal conductor is air $\epsilon_0 = 1$. Figure 2.15 shows cross-section view of coplanar wave-guide media (Pozar, 2012).

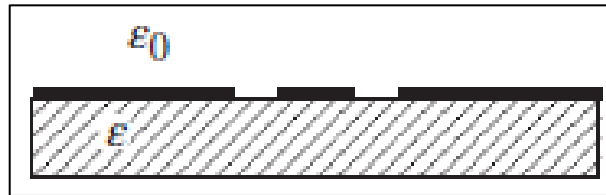


Figure 2.15 Coplanar wave-guide (Edwards & Steer, 2016)

Radiation loss can be a disadvantage as compared to the stripline transmission line. In stripline signal conductor is encapsulated with a uniform dielectric material and ground planes locate at ends. This topology decreases radiation loss as compared to CPW because in CPW topology signal conductor is between the dielectric material and free space as an interface which causes more radiation loss. CPW transmission lines can be realized with traditional PCB realization techniques. Signal conductors in ground planes are easily accessible for connection with other circuit elements and testing measurement is more easily (Pozar, 2012) (Wadell, 1991) (Gupta, Garg, Bahl, & Bhartia, 1996).

As compared to microstrip lines, CPW transmission lines have also both advantages and disadvantages. Only a single layer exists in CPW topology, which both ground planes and signal conductor is placed. Figure 2.16 shows the geometry and naming of geometries.

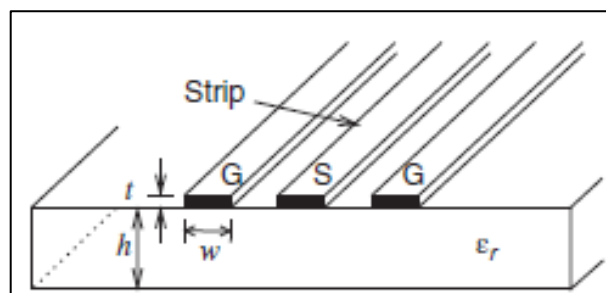


Figure 2.16 Coplanar waveguide geometry (Edwards & Steer, 2016)

This geometry allows easy connection between the ground plane and signal conductor as compared to microstrip lines. Adding distance like the connection between the ground plane and signal conductor causes parasitic inductance. This smaller parasitic inductance exists although the connection is easily between two planes (Edwards & Steer, 2016).

In a theoretical approach, the area of ground planes in the CPW transmission line should extend to infinity. In a practical case, it is applicable and performance discrepancy is negligible if the ground plane is greater three times than the signal width (w). The ground plane places in the CPW transmission line limit the type of coupling that can be used compared to microstrip transmission line topology. For example, end coupled can be achieved with the CPW transmission line but a parallel coupled line cannot be realized because it violated signal conductor and ground plane spacing. This disadvantage limits the usage of CPW transmission lines in microwave structures when the parallel coupling is needed (Pozar, 2012) (Gupta, Garg, Bahl, & Bhartia, 1996) (Wadell, 1991).

2.7.3 Microstrip Line

Microstrip line has one signal-carrying conductor on a top layer. The ground plane is separated by a dielectric material with a uniform dielectric constant ϵ from the signal conductor (Edwards & Steer, 2016).

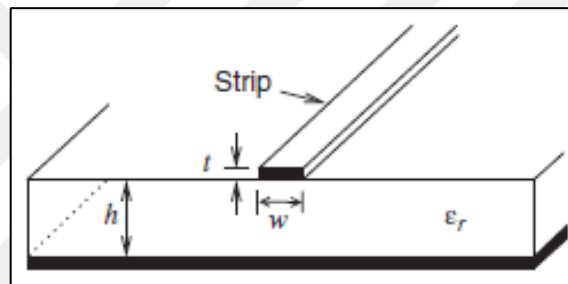


Figure 2.17 Microstrip transmission line (Edwards & Steer, 2016)

t = thickness of conductor

w = width of conductor

h = thickness of dielectric material

ϵ_r = dielectric constant of free space

The signal conductor is surrounded by air, which has $\epsilon_0 = 1$. Figure 2.17 shows cross-section view of microstrip transmission line media. As compared to stripline and CPW lines, microstrip line has suffered significantly more radiation loss like CPW lines. Because similar to CPW, the signal conductor is between the dielectric material and free space as an interface which causes more radiation loss. Like CPW lines, microstrip lines also can be easily realized with simple PCB realization techniques. The signal conductor in microstrip line as compared to stripline is easily accessible for connection with other circuit elements and testing measurement is more easily like CPW (Barrett, 1984) (Pozar, 2012).

Two signal layers are required in a microstrip line topology. As shown in Figure 2.18 signal conductor layer is separated by ground plane layer with a dielectric material and definitions for the naming of geometries are given in Figure 2.18. A signal conductor

has the characteristic impedance Z_0 and its value is controlled by the geometry of the signal conductor. The placing of a ground plane and signal conductor in different layers gives advantages in case of the types of coupling which can be applied (Pozar, 2012) (Edwards & Steer, 2016).

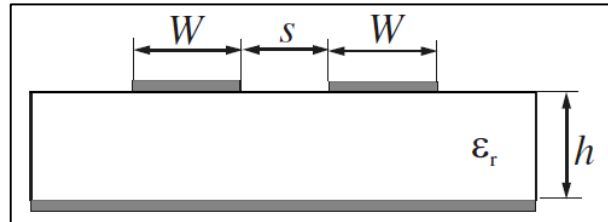


Figure 2.18 Coupled microstrip line (Hong & Lancaster, 2001)

Figure 2.18 shows of cross-sectional view of a simple coupled microstrip line and possible coupling techniques in microstrip lines; parallel coupling and end coupling are given in Figure 2.19. In end coupling, the signal is capacitively coupled across the gap on the microstrip lines. In parallel coupling, the signal is capacitively coupled between the overlapping parallel lines with gaps on the microstrip lines (Mariani & Agrios, 1970) (Wadell, 1991) (Bahl & Trivedi, 1977).

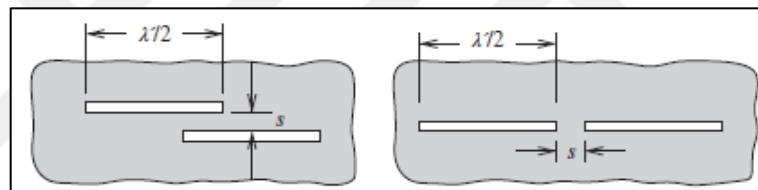


Figure 2.19 Quarter-wave coupled and end coupled microstrip lines (Edwards & Steer, 2016)

The connection can be created with a hole drilled from the signal conductor to the ground plane and filled with a conductive material. This connection is adding distance like CPW lines but it is more difficult to realize connections and cause unwanted parasitic inductances and also effect realization techniques. This connection effect can be reduced by applying different design techniques, which does not use such connections. To sum up all transmission lines, stripline, microstrip line, and CPW transmission lines have some advantages and disadvantages. Table 2.3 summaries some differences between these transmission lines (Edwards & Steer, 2016).

Table 2.3 Attributes comparison of stripline, CPW and microstrip line

Characteristic Attribute	Types of Transmission Line		
	Stripline	CPW	Microstrip
Conductor Layers	3	1	2
Signal Conductor Access	No	Yes	Yes
Realization Using PBC Techniques	No	Yes	Yes

Stripline has an access problem to signal conductor and has a complicated realization technique with three-layer count as compared to microstrip line and CPW.

These problems are decreasing the use of this type of transmission line. The main disadvantage of the CPW line is the limited type of couplings, which are available. The main disadvantage of the microstrip line is the parasitic inductance caused by connections between the ground plane and signal conductor. The main advantage of the microstrip line is lots of different types of coupling can be realized. According to above descriptions; because of versatility in coupling and ease of realization, the microstrip transmission line is the best choice for bandpass filter design (Pozar, 2012).

2.8 Richard's Transformations

According to transformations developed by P.Richard, LC networks can be synthesized using open and short-circuited transmission lines. This transformation relies on a mapping between ω plane to the π plane (Richard, 1948).

In the below equation;

$$\Omega = \tan \beta \ell = \tan\left(\frac{\omega \ell}{v_p}\right) \quad (2.24)$$

Mapping is repeating with a period of $\omega \ell / v_p = 2\pi$. By replacing frequency ω with Ω , the reactance of an inductor can be written as:

$$jX_L = j\Omega L = jL \tan \beta \ell \quad (2.25)$$

And the susceptance of the capacitor can be written as:

$$jB_C = j\Omega C = jC \tan \beta \ell \quad (2.26)$$

For low pass filter prototype cut-off occurs at unity frequency to obtain some result for the Richard's transformed filter.

$$\Omega = 1 = \tan \beta \ell \quad (2.27)$$

Which gives a step length of $\ell = \lambda / 8$. λ wave length of the line at the cut-off frequency (ω_c).

The desired filter prototype response is changed when the frequency increases. The response is periodic when frequency repeats every $4\omega_c$. At the frequency

$\omega_0 = 2\omega_c$, the transmission line is $\lambda/4$ length and an attenuation pole will be added to response (Hong & Lancaster, 2001).

The inductors and capacitors of lumped element filter design can be replaced with short circuit and open circuit stubs as shown in Figure 2.20 (a) and (b).

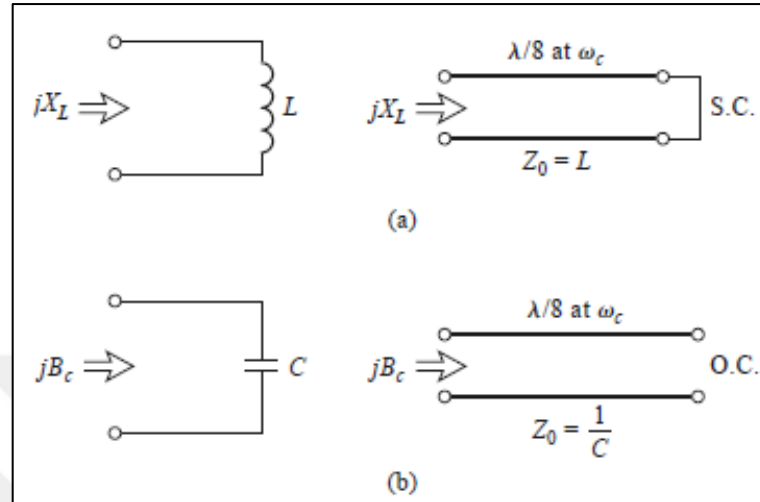


Figure 2.20 (a) Richards transformation for an inductor, (b) for a capacitor (Pojar, 2012)

2.9 Kuroda's Identities

Kuroda identities use $\lambda_c/8$ lengths redundant transmission lines to provide a more applicable microwave filter design by performing any of the following operations.

- 1) Separate shorted or open transmission line stubs physically.
- 2) Transform shunt stubs into series stubs or vice versa.
- 3) Change impractical characteristic impedances into more realizable ones (Pojar, 2012).

Four Kuroda identities are illustrated in Figure 2.21.

In Figure 2.21 each box represents a unit element or transmission line with represented characteristic impedance and length ($\lambda_c/8$ at ω_c). The inductors represent short-circuited stubs and the capacitor represents open circuited stubs. To show the usefulness of Kuroda identities, Richard transformation applied low pass prototype filter circuit can be transformed as an example.

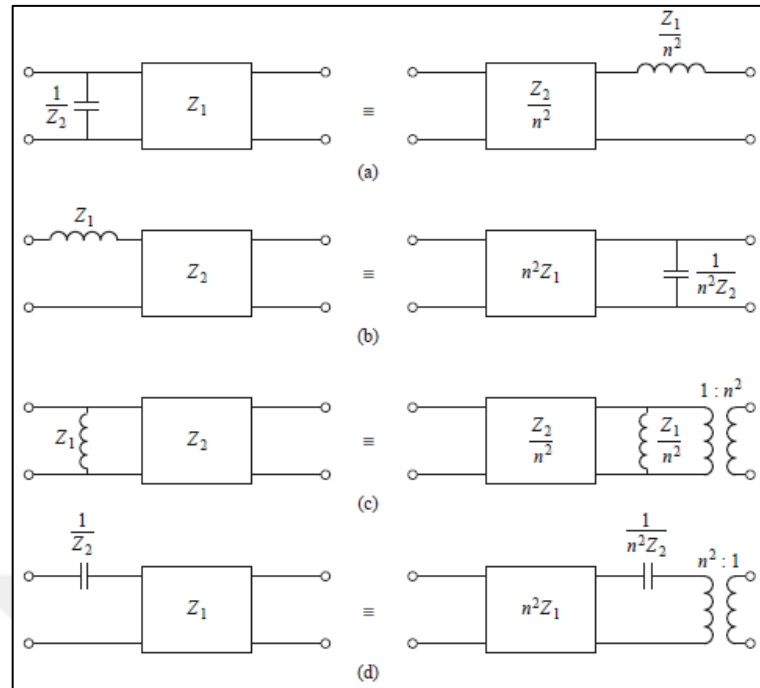


Figure 2.21 Kurado identities (Pozar, 2012)

Before example, first two most useful identities will be discussed. Consider Figure 2.22 (a) two-port network, constructed an open circuit shunt stub and a length of the transmission line as shown in the figure.

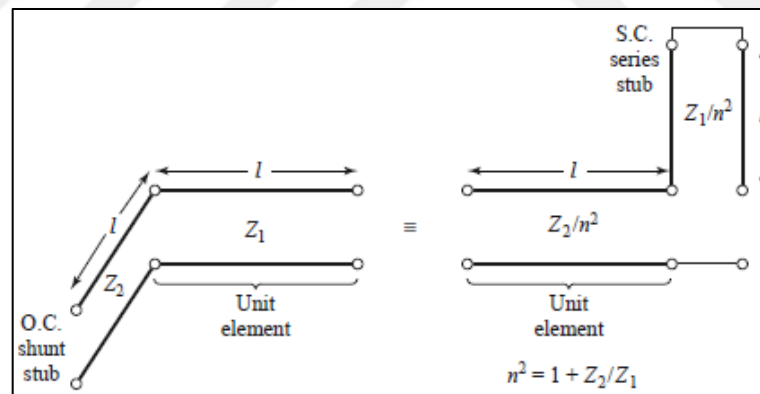


Figure 2.22 Kuroda identity (a) equivalent circuit (Pozar, 2012)

The length of the stub and the transmission line are identical, but the characteristic impedance of each part is different. By using the first Kurado identity equivalent circuit is obtained as shown in Figure 2.22. According to Kuroda identity the two-port network in Figure 2.21 (a) is precisely the same with the two-port network in Figure 2.22 (Pozar, 2012). Thus, applying Kuroda identities, the circuit in Figure 2.22 can be changed to an equivalent circuit using a short-circuited series stub in Figure 2.22 and the behavior of that circuit does not change.

The second Kuroda identity in Figure 2.21 (b) shows a two-port network constructed with a short circuit series stub and a length of a transmission line is shown in below Figure 2.23.

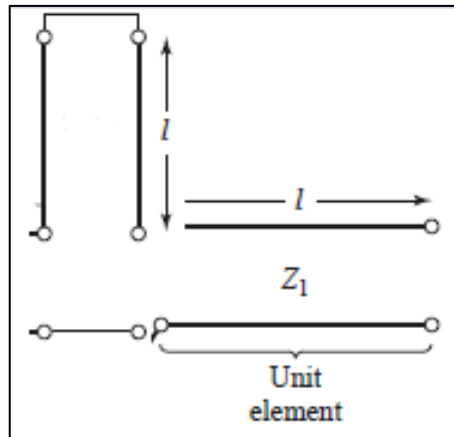


Figure 2.23 Kuroda identity (b) equivalent circuit

By using 2. Kuroda identity, the equivalent circuit is obtained as shown in Figure 2.23. The equivalent circuit uses on open shunt stub. The low pass filter with lumped elements is transformed into distributed elements by applying Richard transformations. But this distributed circuit model has some problems when it is needed to implement. The first problem is, the stubs are ideally infinitely close to each other. They should be separated from each other. Separating needs new transmission lines length between them, which will affect filter response. The second one is, it is difficult to construct series stubs in microstrip. It will be better if all elements are shunt stubs. To solve these problems, the transmission line (Z_0 and $\ell = \lambda/8$) is added to the beginning and end of the filter. Adding these lengths only causes a phase shift in the filter response, the transformer and reflection function remains the same. After that 2. Kurado identity can be applied to replace series stubs with shunts. The realizable filter with three separated shunt stubs is obtained in Figure 2.25 with length and characteristic impedances as labeled.

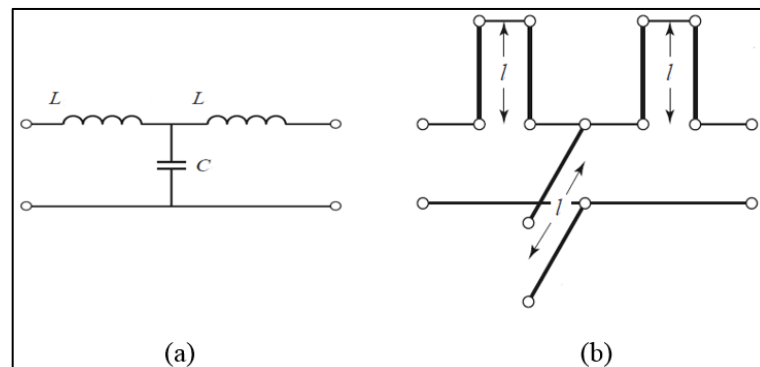


Figure 2.24 (a) Low pass filter with inductors and capacitor, (b) Richard's Transformations applied form (Pozar, 2012) (edited by author)

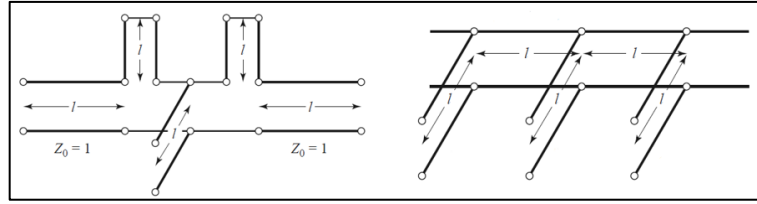


Figure 2.25 Low pass filter 2nd Kuroda identities is applied (Pozar, 2012) (edited by author)

Similar procedures can be used for band-stop filters, but Kuroda identities are not useful for high-pass and band-pass filters (Pozar, 2012).

2.10 Resonator with Transmission Lines

2.10.1 Short-Circuited ($\lambda/4$) Length Transmission Line

Short-circuited $\lambda/4$ length transmission line behaves like a lumped parallel resonator. In Figure 2.26, Z_0 is the characteristic impedance of the line, β is propagation constant and α is attenuation constant.

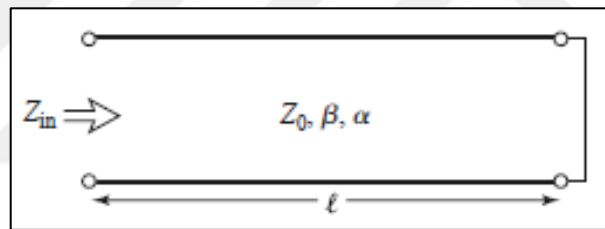


Figure 2.26 Short-circuited $\lambda/4$ length lossy transmission line (Pozar, 2012)

Assume the transmission line is lossless when the length of the transmission line is exactly $\lambda/4$ at w_0 , the input impedance to the line (Z_{in}) is infinite. In case of losses are in accounting the input impedance (Z_{in}) is at a maximum value. The input impedance (Z_{in}) value is changing between a short ($Z_{in}=0$) to an open ($Z_{in}=\infty$) at resonance, this behavior implies this line would be a good reciprocating element. $\lambda/4$ length line can be used as a type of immittance inverter. For the $\lambda/4$ length short-circuited case, if the line length increased at set w_0 , the input impedance (Z_{in}) is increasingly capacitive. As the line length decreases, the input impedance (Z_{in}) is increasingly inductive. Similarly, at a fixed length $\lambda/4$, the input impedance (Z_{in}) is more and more capacitive if w_0 is increase and (Z_{in}) is increasingly inductive as w_0 is decreased (Pozar, 2012).

From similar behavior of a shorted $\lambda/4$ length of line and a parallel lumped resonator circuit, the below relationship can be derived. As assuming that resonator losses are negligible (loss per length is very small).

The input impedance of the parallel RLC circuit;

$$Z_{in} \approx \frac{R}{1 + 2j\theta\Delta\omega / \omega_0} \quad (2.28)$$

And the input impedance of the shorted $\lambda/4$ line is;

$$Z_{in} = \frac{1}{(1/R) + 2j\Delta\omega C} \quad (2.29)$$

Both results are in some form. Then the resistance, inductance, and capacitance of the equal circuit are given below.

Resistance;

$$R = \frac{Z_0}{\alpha\ell} \quad (2.30)$$

Capacitance;

$$C = \frac{\pi}{4\omega_0 Z_0} \quad (2.31)$$

Inductance;

$$L = \frac{1}{\omega_0^2 C} \quad (2.32)$$

2.10.2 Open-Circuited ($\lambda/2$) Length Transmission Line

Open-circuited $\lambda/2$ length transmission line behaves like a lumped parallel resonant circuit. This practical resonator is often used in microstrip circuits. In Figure 2.27, Z_0 is the characteristic impedance of the line, β is propagation constant and α is attenuation constant.

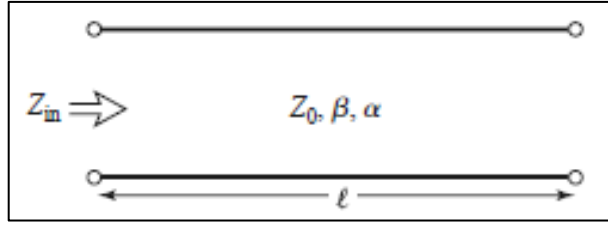


Figure 2.27 Open-circuited $\lambda/2$ length lossy transmission line (Pozar, 2012)

Assuming the transmission line is a lossless $\lambda/2$ length open-circuited line at ω_0 , the input impedance to the line (Z_{in}) is infinite or at a maximum value when losses are taking account.

$\lambda/2$ length line behavior repeats every $n\lambda/2$ where n is any positive integer. When the length is exactly $n\lambda/2$ at ω_c , the performance of the resonator is best and comparable to a parallel lumped resonator.

Comparing Z_{in} of the $\lambda/2$ length resonator in with (Z_{in}) of $\lambda/4$ the short-circuited transmission line in the previous chapter.

$$Z_{in} = \frac{Z_0}{\alpha\ell + j(\Delta\omega\pi/\omega_0)} \quad (2.33)$$

The resistance, capacitance, and inductance of the equivalent circuit can be identified by the below equations.

Resistance;

$$R = \frac{Z_0}{\alpha\ell} \quad (2.34)$$

Capacitance;

$$C = \frac{\pi}{2\omega_0 Z_0} \quad (2.35)$$

Inductance;

$$L = \frac{1}{\omega_0^2 C} \quad (2.36)$$

And unloaded θ is;

$\ell = \pi / \beta$ at resonance.

$$\theta_0 = \omega_0 RC = \frac{\pi}{2\alpha\ell} = \frac{\beta}{2\alpha} \quad (2.37)$$

At frequencies, away from ω_0 distributed resonator performance degrades. The performance similarities between lumped and distributed resonators are only valid at frequencies near ω_0 (the frequency of operation). This performance problem affects the usage of distributed resonators. They are only used when fractional bandwidth requirements are about 15% or less.

2.11 Coupled Line Filters

The parallel coupled transmission lines can be utilized to obtain different types of the filter such as low-pass, band-pass, all-pass and all-stop. The higher order band-pass or band-stop coupled line filters which have bandwidths less than about 20% can be realized in microstrip or stripline form. If the bandwidth of the filter is wider than 20%, it requires very tight coupled lines which is difficult to realize (Bhattacharjee & Singh, 2012).

A two-port network can be created from the coupled line by terminating two of the four parts in either open or short circuits ten possible combinations can be established (Pojar, 2012). As indicated in Table 2.4, various termination causes different frequency responses including low-pass, band-pass, all-pass and all-stop.

Table 2.4 Coupled line circuits with various terminations (Pozar, 2012)

Circuit	Image Impedance	Response
	$Z_{i1} = \frac{2Z_{0e}Z_{0o} \cos \theta}{\sqrt{(Z_{0e} + Z_{0o})^2 \cos^2 \theta - (Z_{0e} - Z_{0o})^2}}$ $Z_{i2} = \frac{Z_{0e}Z_{0o}}{Z_{i1}}$	<p>Low-pass</p>
	$Z_{i1} = \frac{2Z_{0e}Z_{0o} \sin \theta}{\sqrt{(Z_{0e} - Z_{0o})^2 - (Z_{0e} + Z_{0o})^2 \cos^2 \theta}}$	<p>Bandpass</p>
	$Z_{i1} = \frac{\sqrt{(Z_{0e} - Z_{0o})^2 - (Z_{0e} + Z_{0o})^2 \cos^2 \theta}}{2 \sin \theta}$	<p>Bandpass</p>
	$Z_{i1} = \frac{\sqrt{Z_{0e}Z_{0o}} \sqrt{(Z_{0e} - Z_{0o})^2 - (Z_{0e} + Z_{0o})^2 \cos^2 \theta}}{(Z_{0e} + Z_{0o}) \sin \theta}$ $Z_{i2} = \frac{Z_{0e}Z_{0o}}{Z_{i1}}$	<p>Bandpass</p>
	$Z_{i1} = \frac{Z_{0e} + Z_{0o}}{2}$	All pass
	$Z_{i1} = \frac{2Z_{0e}Z_{0o}}{Z_{0e} + Z_{0o}}$	All pass
	$Z_{i1} = \sqrt{Z_{0e}Z_{0o}}$	All pass
	$Z_{i1} = -j \frac{2Z_{0e}Z_{0o}}{Z_{0e} + Z_{0o}} \cot \theta$ $Z_{i2} = \frac{Z_{0e}Z_{0o}}{Z_{i1}}$	All stop
	$Z_{i1} = j \sqrt{Z_{0e}Z_{0o}} \tan \theta$	All stop
	$Z_{i1} = -j \sqrt{Z_{0e}Z_{0o}} \cot \theta$	All stop

According to the realization, advantage of open circuit structures in microstrip, the below figure shows coupled line filter with terminated with open circuits.

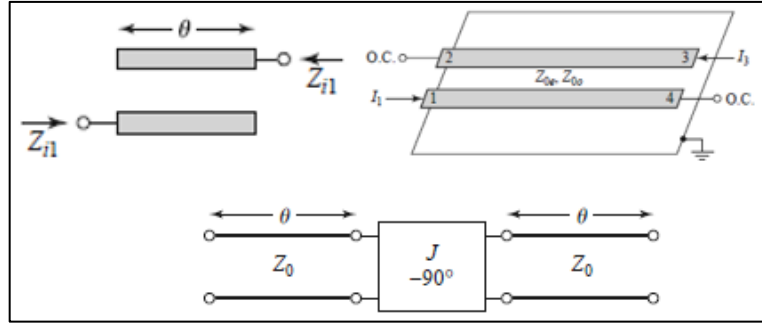


Figure 2.28 Coupled open circuits (Pozar, 2012)

In this type, $I_2 = I_4 = 0$ and four port impedance equations can be updated as below:

$$V_1 = Z_{11}I_1 + Z_{13}I_3 \quad (2.38)$$

$$V_3 = Z_{31}I_1 + Z_{33}I_3 \quad (2.39)$$

Image impedance with Z-parameters is;

$$Z_i = \sqrt{Z_{11}^2 - \frac{Z_{11}Z_{13}^2}{Z_{33}}} \quad (2.40)$$

$$Z_i = \frac{1}{2} \sqrt{(Z_{0e} - Z_{0o})^2 \csc^2 \theta - (Z_{0e} + Z_{0o})^2 \cot^2 \theta} \quad (2.41)$$

When the coupled line is $\lambda / 4$ the length $\theta = \Omega / 2$, the image impedance reduces to

$$Z_i = \frac{1}{2} (Z_{0e} - Z_{0o}) \quad (2.42)$$

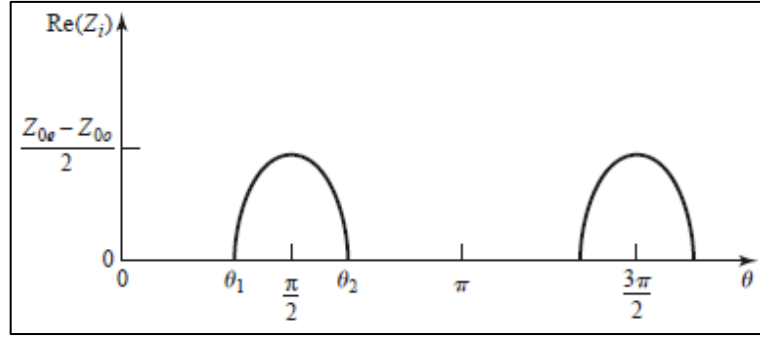


Figure 2.29 Bandpass network image impedance real part

The image impedance Z_i is real and positive since $Z_{0e} > Z_{0o}$ shown in Figure 2.29.

When $\theta \rightarrow 0$ or π , $Z_i \rightarrow \pm\infty$, indicating attenuation.

Cut off frequencies calculated from Z_i

$$\cos \theta_1 = -\cos \theta_2 = \frac{Z_{0e} - Z_{0o}}{Z_{0e} + Z_{0o}} \quad (2.43)$$

The propagation constant;

$$\cos \beta = \sqrt{\frac{Z_{11}Z_{33}}{Z_{13}^2}} = \frac{Z_{11}}{Z_{13}} = \frac{Z_{0e} + Z_{0o}}{Z_{0e} - Z_{0o}} \cos \theta \quad (2.44)$$

Which shows β is real for $\theta_1 < \theta < \theta_2 = \pi - \theta_1$, where $\cos \theta_1 = (Z_{0e} - Z_{0o}) / (Z_{0e} + Z_{0o})$

2.11.1 Admittance Inverters and Coupling in Filter Design

Narrowband band-pass filters can be created with cascaded parallel coupled lines. The relation is important between admittance inverters and coupling between lines. Admittance inverter provides a model for this coupling (Hong & Lancaster, 2001).

In Figure 2.30, two transmission line resonators of length θ are parallel coupled with spacing between lines S and w of the lines. In Figure 2.31 these two θ length transmission line resonators are coupled together by an admittance inverter and form equivalent circuit model (Hong & Lancaster, 2001).

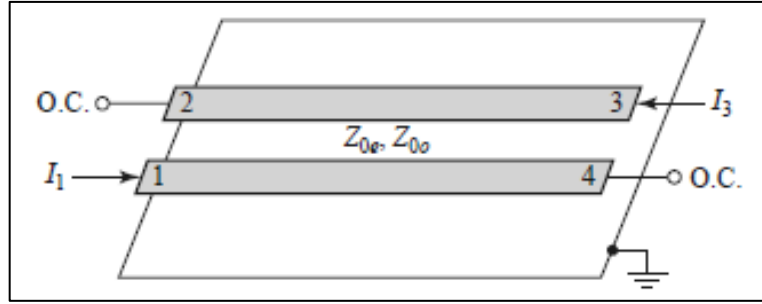


Figure 2.30 Coupled transmission lines (Pozar, 2012)

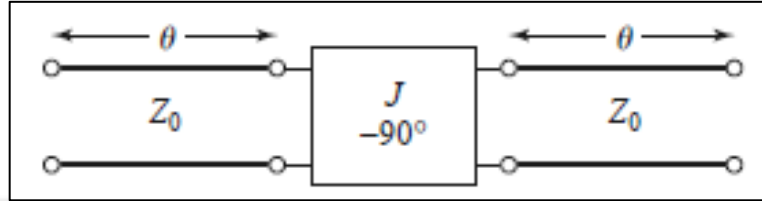


Figure 2.31 Equivalent of the coupled lines in Figure 2.30 (Pozar, 2012)

In Figure 2.32, a parallel coupled line filter of n^{th} order is displayed. There is a coupling section admittance inverter value J related with each coupling section of each individual resonator. In Figure 2.32, the impedance of the generator and load is Z_0 , the line lengths θ are $\lambda/4$ in length at the central frequency. Each section coupling will differ according to filter design specifications. This means the spacing and line widths of each coupled section will effect filter response and to maintain desired response all dimensions have a different value. As a result, each coupled section has different (J) admittance inverter value and the input and output part of admittance inverter constant calculation is different from the interior part (Hong & Lancaster, 2001).

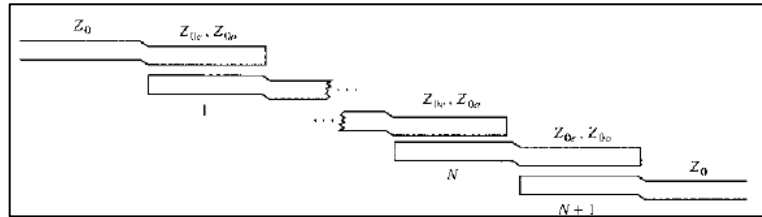


Figure 2.32 n^{th} order parallel coupled line filter (Pozar, 2012)

In below equations, Δ is the fractional bandwidth of the band-pass filter, g_n to g_{n+1} are normalized element values of the low pass filter prototype.

To calculate input section admittance inverter constant;

$$J_{01} \cdot Z_0 = \sqrt{\frac{\pi \cdot \Delta}{2 \cdot g_0 \cdot g_1}} \quad (2.45)$$

To calculate the admittance inverter constant between generator and load sections;

$$J_{ij+1} \cdot Z_0 = \frac{\pi \cdot \Delta}{2\sqrt{g_j \cdot g_{j+1}}} \text{ where } j = 1 \text{ to } n-1 \quad (2.46)$$

To calculate output section admittance inverter constant;

$$J_{n,n+1} \cdot Z_0 = \sqrt{\frac{\pi \cdot \Delta}{2 \cdot g_n \cdot g_{n+1}}} \quad (2.47)$$

Even and odd mode impedances can be calculated with all the values defined in above equations (Pozar, 2012).

First and last equations are only used for symmetrical coupled lines, the characteristic impedance of the filter Z_0 is equal to the individual resonator characteristic impedances Z_R . The asymmetrical coupled lines can be derived because of input and output resonators $Z_0 \neq Z_R$. In this case, using input and output inverters solve this problem. There are also other options to solve this asymmetrical problem like $\lambda/4$ transformers, lumped inverters or applying the input or output at the appropriate location on the first (input) and output (last) resonators to produce the equivalence in filter characteristic impedance Z_0 (Hong & Lancaster, 2001).

Because of the coupling section (inverter port) can have a different admittance inverter value ($J_{01}, J_{12}, \dots, etc$) the even, odd mode impedances Z_{0e} , Z_{0o} of each section may be different.

Previously even and odd mode impedance of a coupled line is calculated relative to the ground when the line is excited by an even or odd mode excitation.

For the calculation of even and odd mode characteristic impedance of resonators in filter based on the admittance inverter ($J_{01}, J_{12}, \dots, etc$) calculated by coupled lines admittance inverters, the below equations are used.

$$(Z_{0e})_{j,j+1} = Z_0(1 + J_{j,j+1}Z_0 + J_{j,j+1}^2Z_0^2) \quad (2.48)$$

$$(Z_{0e})_{j,j+1} = Z_0(1 - J_{j,j+1}Z_0 + J_{j,j+1}^2Z_0^2) \quad (2.49)$$

These even and odd mode characteristic impedances can be used to calculate microstrip filter layout dimensions of line widths and spacing of the parallel coupled lines (Pojar, 2012).

2.11.2 Coupled Line Theory and Even-Odd-Mode Analysis

If two transmission lines are close to each other, electromagnetic fields of each lines interactions cause a power coupling between the lines. These lines are called as coupled transmission lines, and in general consist of three conductors. With close proximity as shown in Figure 2.33. Coupled transmission lines are usually assumed to operate in the TEM mode which is valid for microstrip structures. Supporting two distinct propagating modes gain this three-wire line can be used to implement filters (Pojar, 2012).

Assuming TEM propagation is valid, the effective capacitances between three lines and the velocity of the propagation on the line set the coupled lines' electrical characteristics. Figure 2.33 shows the equivalent capacitance network of three-wire lines. In Figure 2.33, C_{12} symbolizes the capacitance between two strip lines, the capacitance between one strip line and the ground line is shown with C_{11} and C_{22} (Pojar, 2012).

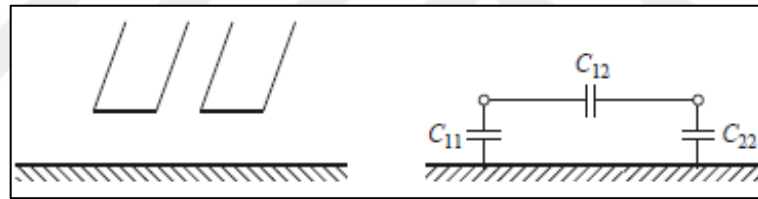


Figure 2.33 Equivalent capacitance network of three-wire lines (Pojar, 2012)

In symmetrical structures, $C_{11} = C_{22}$ which are identical in size and location relative to the ground line. In many applications, the third line is used as a ground plane of a microstrip circuit (Pojar, 2012).

Even and odd modes are two special excitation types of coupled lines. To mention the electrical characteristic of coupled lines, even and odd mode analysis is used. In even and odd mode analysis, it is assumed that lines are symmetric and fringing capacitances are equal for both modes. In Figure 2.34, the even and odd mode excitations of a coupled microstrip line are shown (Hong & Lancaster, 2001).

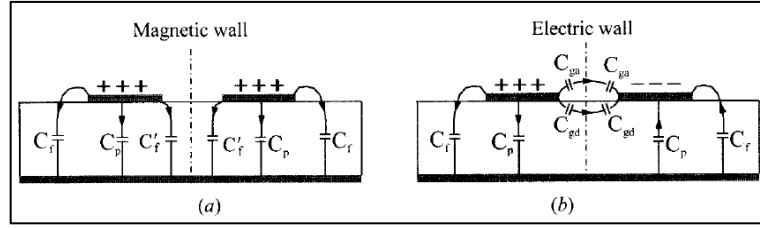


Figure 2.34 Quasi-TEM modes of coupled lines; (a) Even mode excitation (b) Odd mode excitation (Hong & Lancaster, 2001)

In the even mode, the currents in the two lines are equal in amplitude and in the same direction. The even mode excitation creates an electric field which has even symmetry about the center line and is without current flows between two lines, resulting as a magnetic boundary which can be considered as an open circuit. There is not any electric field interaction between lines in even mode. Figure 2.34 (a) shows an updated capacitance network of even mode applied coupled lines (Pozar, 2012) (Hong & Lancaster, 2001).

C_{12} capacitance between lines is replaced with an open circuit. If C_{11} and C_{22} are equal, even mode capacitance C_e is $C_e = C_{11} = C_{22}$.

Assuming two lines are identical in size and location, the characteristic impedance for even mode can be calculated with the below equation:

v_p = velocity of propagation, C_e = even-mode capacitance.

$$Z_{0e} = \sqrt{\frac{L_e}{C_e}} = \frac{\sqrt{L_e C_e}}{C_e} = \frac{1}{v_p C_e} \quad (2.50)$$

where

$$v_p = c/\sqrt{\epsilon_r} = 1/\sqrt{L_e C_e} = 1/\sqrt{L_o C_o} \quad (2.51)$$

In the odd mode, in the two lines, the currents are equal in amplitude and flow in the opposite directions on each line. The odd mode excitation creates an electric field, the symmetry of which is odd about the center line and there is not any voltage difference between the two lines. It can be obtained from assuming a ground plane is exist in the middle of C_{12} . Figure 2.34 (b) shows the equivalent capacitance network off odd mode excitation applied coupled lines (Pozar, 2012) (Hong & Lancaster, 2001).

C_{12} capacitance between lines is replaced with $2C_{12}$ between one line and ground conductor. If C_{11} and C_{22} are equal, odd mode capacitance C_o between either line and ground is

$$C_o = C_{11} + 2C_{12} = C_{22} + 2C_{12} \quad (2.52)$$

And characteristic impedance for odd mode is given in the below equation:

v_p = velocity of propagation, C_o = odd-mode capacitance.

$$Z_{0o} = \frac{1}{v_p C_o} \quad (2.53)$$

Z_{0e} and Z_{0o} is valid for one line relative to the ground when even or odd mode excitation is applied. These characteristic impedances are used to determine many design specifications of parallel coupled line filters such as widths of lines, the spacing between lines and coupling factor of the lines (Pozar, 2012) (Hong & Lancaster, 2001).

For coupled microstrip lines, predefined even mode and odd mode impedance graphs are existing for specific dielectric constants. In Figure 2.35, even and odd mode impedances for symmetric coupled microstrip lines on a substrate with $\epsilon_r = 10$ is shown to determine microstrip dimensions (Quasi TEM Mode) (Yang, Cross, & Drake, 2014).

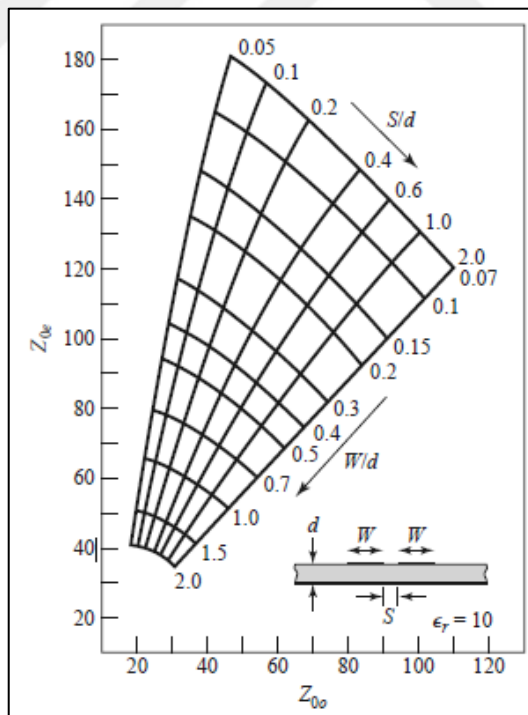


Figure 2.35 Even and odd mode characteristic impedance for symmetric coupled microstrip line on a substrate with $\epsilon_r = 10$ (Pozar, 2012)

2.12 Calculation of Microstrip Dimensions

2.12.1 Akhtarzad's Equations

The Akhtarzad method is based on the even and odd mode impedances (Z_{0e}, Z_{0o}) which are derived by individual coupling sections for example (J_{01}, J_{12}) admittance inverter. The Akhtarzad method gives the ratios for the width to height (W/h) and space to height (s/h) of parallel lines (Akhtarzad, Rowbotham, & Johns, 1975).

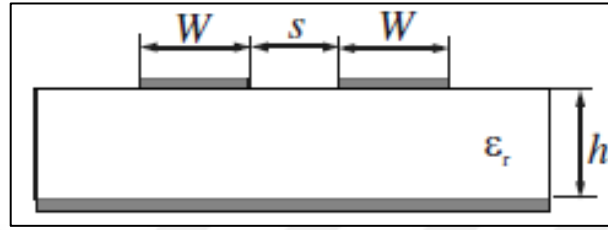


Figure 2.36 Cross-sectional view (Hong & Lancaster, 2001)

Each line has $\lambda/2$ length at central frequencies and overlaps each other by $\lambda/4$ length. $\lambda/4$ length overlap increases the value of coupling and minimizes the required spacing (s) between resonators.

In Figure 2.36, the distance between resonators is illustrated by ' s ', the width of the resonator by ' W ', substrate thickness with ' h ' and the relative dielectric constant at the material with ' ϵ_r '

ϵ_r and h are known as values for a specified substance which is chosen for filter layout. W and s can be determined by using Akhtarzad equations (Akhtarzad, Rowbotham, & Johns, 1975).

Akhtarzad's equations are given below;

$$\left(\frac{W_e}{h}\right) = \frac{2}{\pi} \cosh^{-1}\left(\frac{2h-g+1}{g+1}\right) \quad (2.54)$$

$$\left(\frac{W_o}{h}\right) = \frac{2}{\pi} \cosh^{-1}\left(\frac{2h-g-1}{g-1}\right) + \frac{4}{\pi(1+\epsilon_r/2)} \cosh^{-1}\left(1 + 2\frac{W/h}{s/h}\right) \quad (2.55)$$

where;

$$g = \cosh\left(\frac{\pi \cdot s}{2 \cdot h}\right) \quad (2.56)$$

$$h = \cosh\left(\pi\left(\frac{W}{h} + \frac{s}{2h}\right)\right) \quad (2.57)$$

$$\left(\frac{s}{h}\right) \approx \frac{2}{\pi} \cosh^{-1} \left(\frac{\cosh\left(\frac{\pi \cdot W_o}{2 \cdot h}\right) + \cosh\left(\frac{\pi \cdot W_e}{2 \cdot h}\right) - 2}{\cosh\left(\frac{\pi \cdot W_o}{2 \cdot h}\right) - \cosh\left(\frac{\pi \cdot W_e}{2 \cdot h}\right) - 2} \right) \quad (2.58)$$

h is known as a value, even and odd mode widths (W_e, W_o) can be calculated by using the characteristic impedances $Z_{0e}/2$ and $Z_{0o}/2$. One of the useful methods for this calculation is given below with equations. This method is used to determine the microstrip width from characteristic impedance (Wadell, 1991) (Bahl & Trivedi, 1977).

$$\left(\frac{W}{h}\right) = \left(\frac{8e^A}{e^{2A} - 2}\right) \text{ for } W/h < 2 \quad (2.59)$$

$$\left(\frac{W}{h}\right) = \left(\frac{2}{\pi} \left(B - 1 - \ln(2B - 1) + \frac{\epsilon_r - 1}{2} \left(\ln(B - 1) + 0.39 - \frac{0.61}{\epsilon_r} \right) \right) \right) \quad (2.60)$$

for $W/h > 2$

where;

$$A = \frac{Z_0}{60} \sqrt{\frac{\epsilon_r + 1}{2}} + \frac{\epsilon_r - 1}{\epsilon_r + 1} \left(0.23 + \frac{0.11}{\epsilon_r} \right) \quad (2.61)$$

$$B = \frac{377\pi}{2Z_0\sqrt{\epsilon_r}} \quad (2.62)$$

In the above equations, Z_0 is equal to $Z_{0e}/2$ or $Z_{0o}/2$ depending on which one W_e/h or W_o/h is calculated using Akhtarzad's equations. ϵ_r is also known as a value which is a substrate relative dielectric constant.

By solving the above equations simultaneously or applying iteration with known value (h) substrate thickness, all the geometries of layout can be calculated.

2.12.2 Calculation of Parallel Coupled Line Filters Line Lengths

The line length of parallel coupled filter resonators is generally equal to $\lambda / 2$. The overlap between resonator is $\lambda / 4$. λ is the wavelength of the signal at central frequency. The wavelength is affected by several factors such as dielectric constant (ϵ_r), the velocity of propagation (v_p) and fringing fields at the ends of the lines.

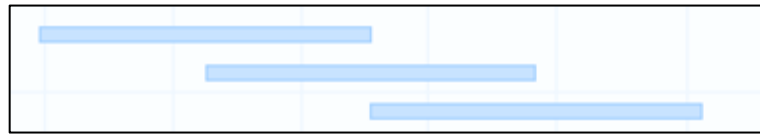


Figure 2.37 Simple display of parallel coupled line filter

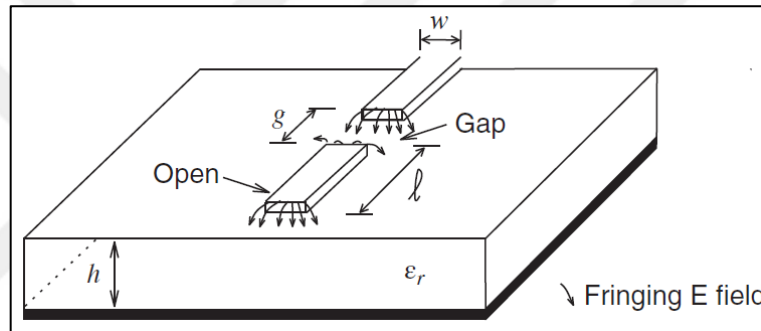


Figure 2.38 Microstrip open circuit and gap layout with electric fields (Edwards & Steer, 2016)

Placing equivalent effective length on simple parallel coupled line filter display (Figure 2.39):

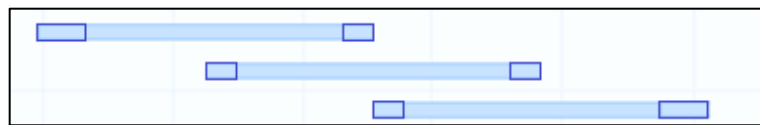


Figure 2.39 Parallel coupled line filter with equivalent effective length

The method for calculating microstrip effective dielectric constant was developed by (Hammerstad & Bekkadal, Microstrip Handbook, 1975). This value will be used later to define effective wavelength (λ_{eff}) at central frequency.

$$\epsilon_f = \frac{\epsilon_r + 1}{2} + \frac{\epsilon_r - 1}{2} \cdot \left(1 + 12 \cdot \frac{h}{w}\right)^{-0.5} \quad (2.63)$$

By applying the below calculation using effective dielectric constant v_p can be calculated.

$$v_p = \frac{c}{\sqrt{\epsilon_{eff}}} \quad (2.64)$$

The effective wavelength can be determined by the below equation:

$$\lambda_{eff} = \frac{v_p}{f} \quad (2.65)$$

According to the Figure 2.38, the line lengths are $\lambda_{eff} / 2$. This length does not take account of fringing fields which is the radiated energy at the end of open lines. This field affects the electrical length of the line. The line seems longer than physical it does. To define the exact value of lengths, the fringing field lengths ℓ_{eo} (equivalent effective length) can be neglected by decreasing physical length. As a simple rule, it is assumed, fringing field adds $h / \sqrt{3}$ length to the line. The more formal method to calculate this value is given in the below equation using effective dielectric constant (Edwards & Steer, 2016) (Hammerstad & Bekkadal, Microstrip Handbook, 1975).

$$\ell_{eo} = 0.412 \cdot h \left(\frac{\epsilon_{eff} + 0.3}{\epsilon_{eff} + 0.258} \right) \cdot \left(\frac{\frac{w}{h} + 0.262}{\frac{w}{h} + 0.813} \right) \quad (2.66)$$

In parallel coupled line filters, all resonators have fringing affects both open ends. The value of this affect is decreased in interior resonators because of flux stolen by adjacent resonators. The equivalent effective length value in interior resonator is $\ell_{eo} / 2$. The aim of calculating equivalent effective length is to determine physical length which is realized because of the equivalent effective length, the electrical length is equal to $\lambda_{eff} / 2$ length but physical length is smaller than the electrically appear (Edwards & Steer, 2016) (Hammerstad & Bekkadal, Microstrip Handbook, 1975).

2.13 Input and Output of a Parallel Coupled Line Filter

The parallel coupled line filters input and output can be obtained from using input and output resonators to apply the signal to the filter.

In this case, the input coupling section admittance is J_{01} and output coupling section admittance is $J_{n,n+1}$ for an n^{th} order filter. However, this solution causes a problem when the filter characteristic impedance Z_0 does not equal to individual resonators characteristic impedance Z_{res} and the equations are invalid for J_{01} and $J_{n,n+1}$ calculations. Because this technique is valid for symmetrical coupled lines.

In asymmetrical coupled lines, several other techniques can be used to obtain input and output of the filter. $\lambda/4$ transformers, lumped inverters and tapping resonators into input and output sections are others choices that can be applied. In the below section tapped line technique is discussed.

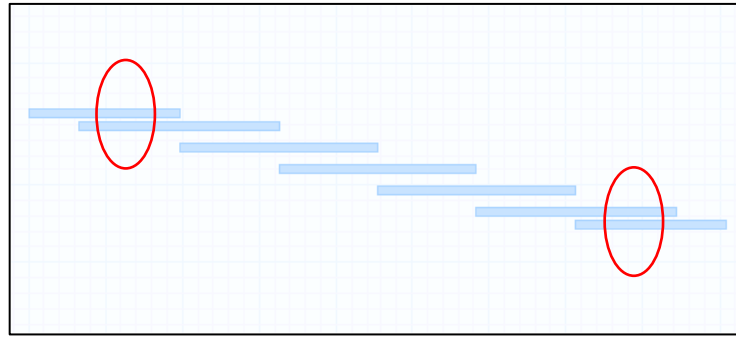
2.13.1 Tapped Line Technique

The tapped line technique can be used to couple lines which have asymmetrical coupling to solve input and output impedance matching problem. This technique was originally introduced by Dishal for use with round-rod interdigital filters (Dishal, 1965).

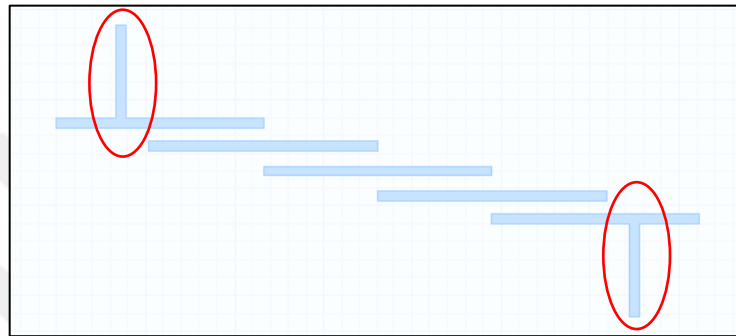
Cristal is applied the same technique in other topologies like stripline, microstrip line, etc. and Wang applied this technique to parallel coupled lines and to hairpin lines (Cristal, 1975). In this technique input and output is created over first and last resonators and this gives space-saving advantage over standard parallel coupled line input and output creation (Wong, 1979).

In Figure 2.40 (a), standard 5th order parallel coupled line filter is given. In the case of tapped line technique usage, there is no need to use input (0) and output (n+1) resonators. As shown in Figure 2.40 (b), taps are directly applied to first (1) and last (n) resonators of the filter (Tsai, 2007).

In $\lambda/2$ length resonator, the voltage and current are changing sinusoidal along the length of the line. This sinusoidal variation causes a very range of impedances. At the open ends very high impedances are obtained and in the middle very low, impedance, which is nearly zero, is obtained. In this case, applying tap to the correct distance in the resonator will yield an impedance match between the filter characteristic impedance Z_0 and individual resonator impedance Z_{res} .



(a)



(b)

Figure 2.40 (a) Standard 5th order parallel coupled bandpass filter, (b) tapped input/output

The tap can be located in only distance ℓ away from the middle of the resonator. To determine the location of the tap, defining the singly loaded Q_{SL} is needed.

$$Q_{SL} = \frac{g_i \cdot f_0}{\Delta} \quad (2.67)$$

g_i = input and output normalized coefficient of the low pass prototype.

f_o = frequency of operation.

Δ = bandwidth in terms of frequency.

Using the below equation and the value of Q_{SL} which is calculated with the above equations. ℓ the tap distance from the middle of the resonator can be calculated (Hong & Lancaster, 2001) (Wong, 1979).

$$\frac{Q_{SL}}{Z_0 / Z_{res}} = \frac{\pi}{2 \sin^2 \left(\frac{\pi \cdot \ell}{2 \cdot L} \right)} \quad (2.68)$$

SECTION 3. PARALLEL COUPLED MICROSTRIP BANDPASS FILTER DESIGN

According to the application which the filter is used, a set of filter specifications can be given or the input signal of the filter defines filter specifications. To use in NR 5G wireless communication applications, a bandpass filter is designed and optimized at a center frequency of 3.5 GHz via the use of Applied Wave Research (AWR) Design Environment (13.03r) software. Chebyshev low pass prototype is used to design a filter with lumped elements and transformations are applied. The realization of the filter is performed, using a microstrip parallel coupled line technique with the implementation of Rogers RO4350 substrate. The bandpass filter design and performance are presented and discussed in the following sections. For the following design, Table 3.1 defines the filter specifications.

Table 3.1 Target filter specifications

Specifications	Value
Center Frequency	3.5 GHz
Bandwidth	200 MHz
Low Pass Prototype	Chebyshev
Passband Ripple	0.5 dB
Filter Order	5th
I/O Impedance	50 ohm
Stopband Attenuation at 3.8 GHz	>-40 dB

3.1 Bandpass Filter Design

3.1.1 Chebyshev Low Pass Filter Prototype

According to filter design, stopband attenuation at 3.8 GHz specification the order of the filter is defined with below calculation and attenuation versus normalized frequency graph for 0.5 dB ripple Chebyshev low pass filter prototype Figure 3.1. The filter order is decided as five (5). The related normalized values of Chebyshev low pass prototype with 0.5 dB ripple in the passband are given in below Table 3.2. These values are used to design a lumped element low pass filter prototype.

$$f_1 = 3400\text{MHz} \quad f_0 = 3500\text{MHz} \quad f_2 = 3600\text{MHz} \quad f_c = 3800\text{MHz}$$

$$f_0 = \sqrt{f_1 \cdot f_2} = (3.49857 \cdot 10^9) \cdot \frac{1}{s} \text{ MHz} \quad (3.1)$$

$$FBW = \frac{f_2 - f_1}{f_0} = 0.057166 \quad (3.2)$$

$$f_n = \frac{1}{FBW} \cdot \left(\frac{f_1}{f_c} - \frac{f_c}{f_1} \right) = -3.8993 \quad (3.3)$$

$$\text{Normalized frequency} = \left| \frac{f_n}{1} \right| - 1 = 2.8993 \quad (3.4)$$

According to the graph order of the filter is decided as five (5).

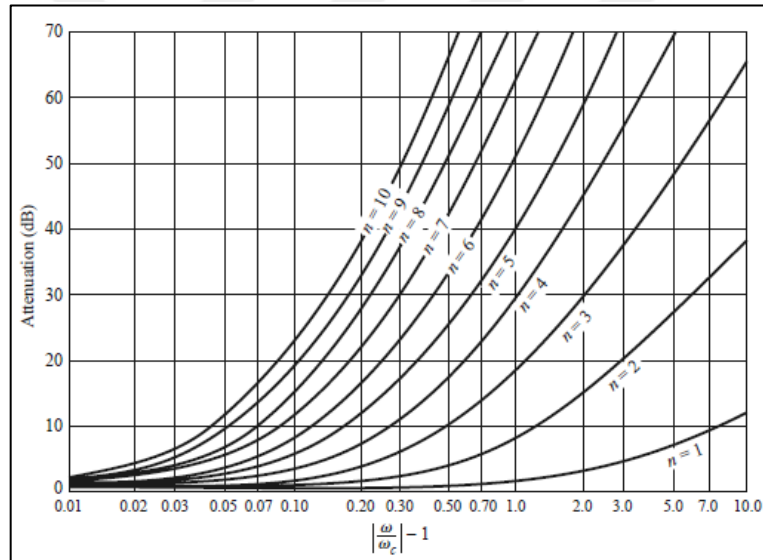


Figure 3.1 Attenuation / normalized frequency; 0.5 dB ripple Chebyshev low pass filter prototype (Pozar, 2012)

Table 3.2 Chebyshev low pass filter prototypes element values for 0.5 dB ripple (Matthaei, Young, & Jones, 1980)

0.5 dB ripple						
Order (n)	g_1	g_2	g_3	g_4	g_5	g_6
1	0.6986	1				
2	1.4029	0.7071	1.9841			
3	1.5963	1.0967	1.5963	1		
4	1.6703	1.1926	2.3661	0.8419	1.9841	
5	1.7058	1.2296	2.5408	1.2296	1.7058	1

Chebyshev type filter with the number of orders, n is chosen as five (5). Using normalized elements “ g_n ” values in Table 3.2, the 5th order low pass prototype circuit is created in Figure 3.2, pi-network is chosen as a lumped element network topology.

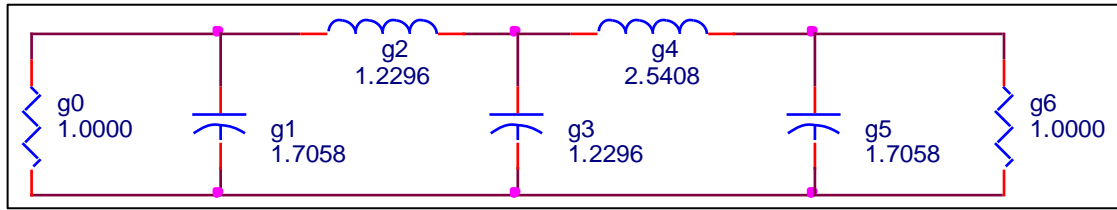


Figure 3.2 5th order low pass prototype circuit

3.1.2 Bandpass Transformation

From the low pass to bandpass transformed topology is shown in below Figure 3.3. The shunt L (inductor) is transformed into series L (inductor) and series C (capacitance) with new values. The shunt C (capacitance) is transformed to shunt L (inductor) and shunt C (capacitance) with new values.

Fractional Bandwidth;
$$\Delta = \frac{w_1 - w_2}{w_0} \quad (3.5)$$

$$L \gg L' = \frac{L}{w_0 \Delta}, \quad C' = \frac{\Delta}{w_0 L} \quad (3.6)$$

$$C \gg L' = \frac{\Delta}{w_0 \cdot C}, \quad C' = \frac{C}{w_0 \Delta} \quad (3.7)$$

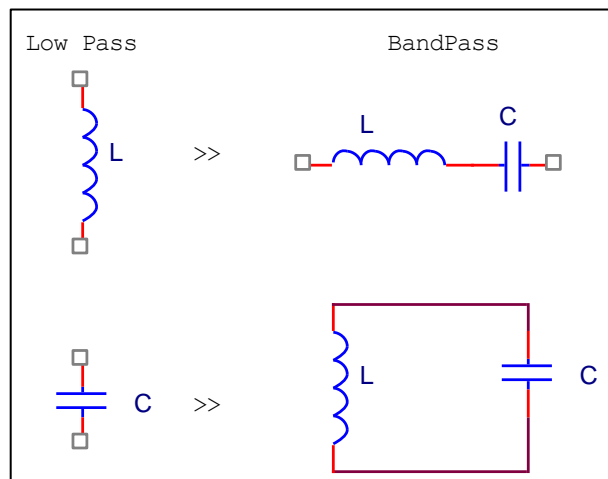


Figure 3.3 Low pass prototype to bandpass transformation

The related calculation is applied to the low pass prototype filter normalized elements in Figure 3.2 and results are given below. Figure 3.4 shows a filter circuit with

element values after bandpass transformation is applied. Figure 3.4 shows the bandpass filter and the element values are given in Table 3.3. The circuit element values of the 5th order bandpass filter are used to calculate of admittance inverters, even-odd mode impedances.

Normalized element values;

$$g_0 = 1.0000 \quad g_1 = 1.7058 \quad g_2 = 1.2296 \quad g_3 = 2.5408 \quad g_4 = 1.2296 \quad g_5 = 1.7058$$

$$g_6 = 1.0000$$

$$Z_0 = 50\Omega \quad f_1 = 3400\text{MHz} \quad f_0 = 3500\text{MHz} \quad f_2 = 3600\text{MHz}$$

$$w_1 = 2\pi \cdot f_1, w_2 = 2\pi \cdot f_2 \quad (3.8)$$

$$w_0 = \sqrt{w_1 \cdot w_2} \quad (3.9)$$

$$\Delta = \frac{w_2 - w_1}{w_0} \quad (3.10)$$

$$C_1 = \frac{g_1}{w_0 \Delta Z_0} = (2.715 \cdot 10^{-11})F \quad (3.11)$$

$$L_1 = \frac{\Delta Z_0}{w_0 g_1} = (7.623 \cdot 10^{-11})H$$

$$C_2 = \frac{\Delta}{w_0 g_2 Z_0} = (4.23 \cdot 10^{-14})F \quad (3.12)$$

$$L_2 = \frac{g_2 Z_0}{w_0 \Delta} = (4.892 \cdot 10^{-8})H$$

$$C_3 = \frac{g_3}{w_0 \Delta Z_0} = (4.044 \cdot 10^{-11})F \quad (3.13)$$

$$L_3 = \frac{\Delta Z_0}{w_0 g_3} = (5.118 \cdot 10^{-11})H$$

$$C_4 = \frac{\Delta}{\omega_0 g_4 Z_0} = (4.23 \cdot 10^{-14}) F \quad (3.14)$$

$$L_4 = \frac{g_4 Z_0}{\omega_0 \Delta} = (4.892 \cdot 10^{-8}) H$$

$$C_5 = \frac{g_5}{\omega_0 \Delta Z_0} = (2.715 \cdot 10^{-11}) F \quad (3.15)$$

$$L_5 = \frac{\Delta Z_0}{\omega_0 g_5} = (7.623 \cdot 10^{-11}) H$$

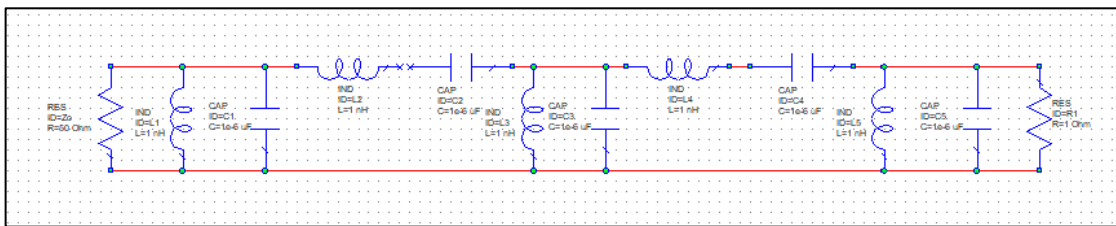


Figure 3.4 5th order bandpass filter with lumped elements

Table 3.3 Capacitor and inductor values of 5th order bandpass filter

C_1	L_1	C_2	L_2	C_3	L_3	C_4	L_4	C_5	L_5
27pF	76pH	42fF	49nH	40pF	51pH	42fF	49nH	27pF	76pH

3.1.3 Admittance Inverters and Even – Odd Mode Impedance

Calculation

Admittance inverters has an important role to transform the lumped element filter into an equivalent form that can be performed using a parallel couple line microstrip structure (Edwards & Steer, 2016).

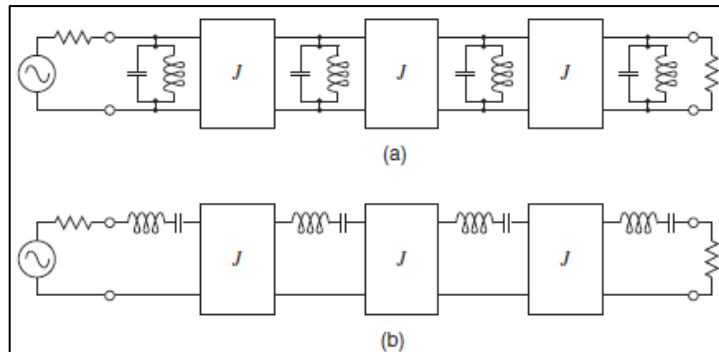


Figure 3.5 Bandpass prototype filter with admittance inverters: (a) shunt resonators (b) series resonators

Figure 3.5 shows a bandpass prototype filter with shunt resonators and admittance inverters. Intermediate coupling structures; admittance inverters values can be calculated with the below equations (Edwards & Steer, 2016). The admittance inverters and even-odd mode impedance calculations are given below. The calculated admittance inverters and even-odd mode impedance values are given in below Table 3.4.

$$\left. \frac{J_{j,j+1}}{Y_0} \right|_{j=1}^{n-1} = \frac{\pi \cdot \Delta}{2 \cdot w_1' \cdot \sqrt{g_j g_{j+1}}} \quad (3.16)$$

First coupling section; $Z_0 J_{01} = \sqrt{\frac{\pi \cdot FBW}{2 \cdot g_0 \cdot g_1}} = 0.229438$ (3.17)

Middle coupling sections;

$$Z_0 J_{12} = \frac{\pi \cdot FBW}{2} \cdot \frac{1}{\sqrt{g_1 \cdot g_2}} = 0.062003 \quad (3.18)$$

$$Z_0 J_{23} = \frac{\pi \cdot FBW}{2} \cdot \frac{1}{\sqrt{g_2 \cdot g_3}} = 0.050803 \quad (3.19)$$

$$Z_0 J_{34} = \frac{\pi \cdot FBW}{2} \cdot \frac{1}{\sqrt{g_3 \cdot g_4}} = 0.050803 \quad (3.20)$$

$$Z_0 J_{45} = \frac{\pi \cdot FBW}{2} \cdot \frac{1}{\sqrt{g_4 \cdot g_5}} = 0.062003 \quad (3.21)$$

Last coupling section; $Z_0 J_{56} = \sqrt{\frac{\pi \cdot FBW}{2 \cdot g_5 \cdot g_6}} = 0.229438$ (3.22)

Even Mode Impedances;

$$\begin{aligned}
 Z_{0e1} &= 50 \cdot (1 + Z_0 J_{01} + (Z_0 J_{01})^2) = 64.104 \\
 Z_{0e2} &= 50 \cdot (1 + Z_0 J_{12} + (Z_0 J_{12})^2) = 53.292 \\
 Z_{0e3} &= 50 \cdot (1 + Z_0 J_{23} + (Z_0 J_{23})^2) = 52.669 \\
 Z_{0e4} &= 50 \cdot (1 + Z_0 J_{34} + (Z_0 J_{34})^2) = 52.669 \\
 Z_{0e5} &= 50 \cdot (1 + Z_0 J_{45} + (Z_0 J_{45})^2) = 53.292 \\
 Z_{0e6} &= 50 \cdot (1 + Z_0 J_{56} + (Z_0 J_{56})^2) = 64.104
 \end{aligned} \tag{3.23}$$

Odd Mode Impedances;

$$\begin{aligned}
 Z_{0o1} &= 50 \cdot (1 - Z_0 J_{01} + (Z_0 J_{01})^2) = 41.1602 \\
 Z_{0o2} &= 50 \cdot (1 - Z_0 J_{12} + (Z_0 J_{12})^2) = 47.0921 \\
 Z_{0o3} &= 50 \cdot (1 - Z_0 J_{23} + (Z_0 J_{23})^2) = 47.5889 \\
 Z_{0o4} &= 50 \cdot (1 - Z_0 J_{34} + (Z_0 J_{34})^2) = 47.5889 \\
 Z_{0o5} &= 50 \cdot (1 - Z_0 J_{45} + (Z_0 J_{45})^2) = 47.0921 \\
 Z_{0o6} &= 50 \cdot (1 - Z_0 J_{56} + (Z_0 J_{56})^2) = 41.1602
 \end{aligned} \tag{3.24}$$

Table 3.4 Calculated parallel coupled line bandpass filter parameters

Parallel Coupled	Admittance Inverter	Even Mode Impedance Z_e	Odd Mode Impedance Z_o
1	0.2294	64.10	41.16
2	0.0620	53.29	47.09
3	0.0508	52.66	47.58
4	0.0508	52.66	47.58
5	0.0620	53.29	47.09
6	0.2294	64.10	41.16

3.1.4 Parallel Coupled Microstrip Dimensions Calculation

In this design RO4350 with a dielectric constant $\epsilon_r = 3.48$ is chosen as substrate material. Substrates are playing very important role in filter performance also affect the cost of realization. Smaller microstrip filters can be designed and realized by using higher dielectric constant materials as substrate (Microwave Journal, 2019). The Rogers RO4350 substrate specifications are stated below Table 3.5.

Table 3.5 Rogers RO4350 substrate specifications

Property	Value
Conductor thickness	0.07mm
Height (h)	0.51mm
Dielectric Constant (ϵ_r)	3.48
Loss Tangent tan g	0.0031

By using the RO4350 substrate with specifications given in Table 3.5 and the calculated even, odd mode parameters in Table 3.4, the dimensions of parallel coupled lines w (width) and s (spacing) can be calculated for desired impedances. Firstly, determine the equivalent single microstrip shape ratios $\frac{w}{h}$. The relation of the coupled line ratios with a single line ratio is used to find the dimensions of coupled microstrip lines that exhibit the desired even mode and odd-mode impedances.

50 ohm line $\frac{w}{h}$ calculation;

$$Z_c = 50 \quad \epsilon_r = 3.48 \quad h = 0.51$$

For $w/h < 2$;

$$A = \frac{Z_c}{60} \cdot \sqrt{\frac{(\epsilon_r + 1)}{2}} + \frac{(\epsilon_r - 1)}{(\epsilon_r + 1)} \cdot (0.23 + \frac{0.11}{\epsilon_r}) = 1.392 \quad (3.25)$$

$$\frac{w}{h} = \frac{8 \cdot e^A}{e^{2A} - 2} = 2.26892 \quad (3.26)$$

$$w = \frac{w}{h} \cdot h = 1.157 \quad (3.27)$$

For $w/h > 2$;

$$B = 377 \cdot \frac{\pi}{2 \cdot Z_c \cdot \sqrt{\epsilon_r}} = 6.34895 \quad (3.28)$$

$$\frac{w}{h} = \frac{2}{\pi} \cdot (B - 1 - \ln(2 \cdot B - 1)) + \left(\frac{\epsilon_r - 1}{2 \cdot \epsilon_r} \right) \cdot (\ln(B - 1) + 0.39 - \frac{0.61}{\epsilon_r}) = 2.26863 \quad (3.29)$$

Wavelength (λ) Calculation of 50 ohm line with e_r ;

$$f = 3.5 \cdot 10^6 \quad e_r = 3.48$$

$$\lambda = \frac{3 \cdot 10^8}{f \cdot e_r} = 24.63054 \quad (3.30)$$

$$L = \frac{\lambda}{4} = 6.1576mm \quad (3.31)$$

The length of the microstrip line is calculated below (Pojar, 2012). Before wavelength calculation, the effective dielectric constant is calculated with an equation which is developed by Bekkadal (Hammerstad, Equations for microstrip circuit design, 1975) (Hammerstad & Bekkadal, 1975).

Bekkadal equation;

Wavelength (λ) Calculation of 50 ohm line with e_f ;

$$f = 3.5 \cdot 10^6 \quad e_r = 3.48 \quad h = 0.51mm$$

$$w = \frac{w}{h} \cdot h = 1.157 \quad (3.32)$$

$$e_f = \frac{e_r + 1}{2} + \frac{e_r - 1}{2} \cdot \left(1 + 12 \cdot \frac{h}{w}\right)^{-0.5} = 2.734 \quad (3.33)$$

$$\lambda = \frac{3 \cdot 10^8}{f \cdot \sqrt{e_f}} = 51.83427 \quad (3.34)$$

$$L = \frac{\lambda}{4} = 12.9586mm \quad (3.35)$$

1st & 6th Coupled line calculation;

Even part w/h calculation;

$$e_r = 3.48 \quad h = 0.51mm$$

$$Z_{0se} = \frac{Z_{0e1}}{2} = 32.052 \quad (3.36)$$

For $w/h < 2$;

$$A = \frac{Z_{0se}}{60} \cdot \sqrt{\frac{(e_r + 1)}{2}} + \frac{(e_r - 1)}{(e_r + 1)} \cdot \left(0.23 + \frac{0.11}{e_r}\right) = 0.9443 \quad (3.37)$$

$$\frac{w}{h} = \frac{8 \cdot e^A}{e^{2A} - 2} = 4.461218 \quad (3.38)$$

For $w/h > 2$;

$$B = 377 \cdot \frac{\pi}{2 \cdot Z_c \cdot \sqrt{e_r}} = 9.90413 \quad (3.39)$$

$$\frac{w}{h} = \frac{2}{\pi} \cdot \left(B - 1 - \ln(2 \cdot B - 1) + \left(\frac{e_r - 1}{2 \cdot e_r} \right) \cdot \left(\ln(B - 1) + 0.39 - \frac{0.61}{e_r} \right) \right) = 4.34521 \quad (3.40)$$

Odd part w/h calculation;

$$e_r = 3.48 \quad h = 0.51mm$$

$$Z_{0so} = \frac{Z_{0o1}}{2} = 20.5801 \quad (3.41)$$

For $w/h < 2$;

$$A = \frac{Z_{0so}}{60} \cdot \sqrt{\frac{(e_r + 1)}{2}} + \frac{(e_r - 1)}{(e_r + 1)} \cdot \left(0.23 + \frac{0.11}{e_r}\right) = 0.6582 \quad (3.42)$$

$$\frac{w}{h} = \frac{8 \cdot e^A}{e^{2A} - 2} = 8.931762 \quad (3.43)$$

For $w/h > 2$;

$$B = 377 \cdot \frac{\pi}{2 \cdot Z_c \cdot \sqrt{e_r}} = 15.42497 \quad (3.44)$$

$$\frac{w}{h} = \frac{2}{\pi} \cdot (B - 1 - \ln(2 \cdot B - 1) + (\frac{e_r - 1}{2 \cdot e_r}) \cdot (\ln(B - 1) + 0.39 - \frac{0.61}{e_r})) = 7.67528 \quad (3.45)$$

Remaining coupled line single microstrip shape ratios $\frac{w}{h}$ are calculated with same equations given above and values are given in Table 3.6.

Table 3.6 Calculated w/h dimensions of transmission lines

Line Description	Even Mode		Odd Mode	
	$w/h < 2$	$w/h > 2$	$w/h < 2$	$w/h > 2$
Coupled Line 1	4.46	4.34	8.93	7.67
Coupled Line 2	5.89	5.54	7.15	6.49
Coupled Line 3	6.00	5.63	7.03	6.40
Coupled Line 4	6.00	5.63	7.03	6.40
Coupled Line 5	5.89	5.54	7.15	6.49
Coupled Line 6	4.46	4.34	8.93	7.67

After single microstrip shape ratios w/h calculation, coupled line ratio relate with single line ratio calculations are given below for s/h and w/h dimensions (Akhtarzad, Rowbotham, & Johns, 1975).

s/h calculation;

$$\frac{s}{h} = \frac{2}{\pi} \cdot \cosh^{-1} \theta \left[\frac{\cosh\left(\left(\frac{\pi}{2}\right) \cdot \left(\frac{w}{h}\right)_{so}\right) + \cosh\left(\left(\frac{\pi}{2}\right) \cdot \left(\frac{w}{h}\right)_{se}\right) - 2}{\cosh\left(\left(\frac{\pi}{2}\right) \cdot \left(\frac{w}{h}\right)_{so}\right) + \cosh\left(\left(\frac{\pi}{2}\right) \cdot \left(\frac{w}{h}\right)_{se}\right)} \right] \quad (3.46)$$

For 1st & 6th coupled line s/h calculation for $w/h < 2$;

$$\left(\frac{w}{h}\right)_{so} = 8.931762; \quad \left(\frac{w}{h}\right)_{se} = 4.461218 \quad (3.47)$$

$$\frac{s}{h} = \frac{2}{\pi} \cdot \cosh^{-1} \theta \left[\frac{\cosh\left(\left(\frac{\pi}{2}\right) \cdot \left(\frac{w}{h}\right)_{so}\right) + \cosh\left(\left(\frac{\pi}{2}\right) \cdot \left(\frac{w}{h}\right)_{se}\right) - 2}{\cosh\left(\left(\frac{\pi}{2}\right) \cdot \left(\frac{w}{h}\right)_{so}\right) + \cosh\left(\left(\frac{\pi}{2}\right) \cdot \left(\frac{w}{h}\right)_{se}\right)} \right] = 0.038 \quad (3.48)$$

$$s_1 = \frac{s}{h} \cdot h = 0.019 \quad (3.49)$$

For 1st & 6th coupled line s/h calculation for $w/h > 2$;

$$\left(\frac{w}{h}\right)_{so} = 7.67528 ; \left(\frac{w}{h}\right)_{se} = 4.34521 \quad (3.50)$$

$$\frac{s}{h} = \frac{2}{\pi} \cdot \cosh^{-1} \theta \left[\frac{\cosh\left(\left(\frac{\pi}{2}\right) \cdot \left(\frac{w}{h}\right)_{so}\right) + \cosh\left(\left(\frac{\pi}{2}\right) \cdot \left(\frac{w}{h}\right)_{se}\right) - 2}{\cosh\left(\left(\frac{\pi}{2}\right) \cdot \left(\frac{w}{h}\right)_{so}\right) + \cosh\left(\left(\frac{\pi}{2}\right) \cdot \left(\frac{w}{h}\right)_{se}\right)} \right] = 0.0932 \quad (3.51)$$

w/h calculation for ;

$$\frac{w}{h} = \frac{1}{\pi} \left(\cosh^{-1} \frac{1}{2} \left(\cosh\left(\frac{\pi s}{2h}\right) - 1 \right) + \left(\cosh\left(\frac{\pi s}{2h}\right) + 1 \right) \cosh\left(\left(\frac{\pi}{2}\right) \left(\frac{w}{h}\right)_{se}\right) \right) - \left(\frac{\pi s}{2h}\right) \quad (3.52)$$

For 1st & 6th coupled line w/h calculation for $w/h < 2$;

$$\left(\frac{w}{h}\right)_{se} = 4.461218 \quad (3.53)$$

$$\frac{w}{h} = \frac{1}{\pi} \left(\cosh^{-1} \frac{1}{2} \left(\cosh\left(\frac{\pi}{2} \cdot 0.038\right) - 1 \right) + \left(\cosh\left(\frac{\pi}{2} \cdot 0.038\right) + 1 \right) \cosh\left(\left(\frac{\pi}{2}\right) \cdot 4.461218\right) \right) - \left(\frac{\pi}{2} \cdot 0.038\right) = 2.212 \quad (3.54)$$

$$w_1 = \frac{w}{h} \cdot h = 1.128 \quad (3.55)$$

For 1st & 6th coupled line w/h calculation for $w/h > 2$;

$$\left(\frac{w}{h}\right)_{se} = 4.34521 \quad (3.56)$$

$$\frac{w}{h} = \frac{1}{\pi} \left(\cosh^{-1} \frac{1}{2} \left(\cosh\left(\frac{\pi}{2} \cdot 0.0932\right) - 1 \right) + \cosh\left(\frac{\pi}{2} \cdot 0.0932\right) + 1 \right) \cosh\left(\left(\frac{\pi}{2}\right) \cdot 4.34521\right) - \left(\frac{\pi}{2} \cdot 0.0932\right) \right) = 2.128 \quad (3.1)$$

In the above equations, 1st and 6th coupled line s/h and w/h dimensions are calculated. Remaining coupled line dimensions are also calculated with the same equations and all dimensions are given in the below table.

Table 3.7 Parallel coupled microstrip dimensions

Line Description	W (mm)	S (mm)	L (mm)
50 ohm Line	1.157	-	6.158
Coupled Line 1	1.128	0.019	12.971
Coupled Line 2	1.401	0.254	12.863
Coupled Line 3	1.412	0.31	12.859
Coupled Line 4	1.412	0.31	12.859
Coupled Line 5	1.401	0.254	12.863
Coupled Line 6	1.128	0.019	12.971

Calculations are made above and the source of these formulas is given in the previous section literature review. First of all, with the above equations, microstrip resonator dimensions are calculated and after that AWR simulation software is used for better filter design and simulation. The steps of filter design using simulation software and the realized filter measurements are given in the following sections.

3.1.5 Simulation of Parallel Coupled Microstrip Bandpass Filter

AWR, iFilter wizard is used to calculate parallel coupled lines dimensions and spacing between two lines and to simulate a designed filter. During design, PCB specifications are set for Rogers RO4350 two-layer substrate with 2oz copper both sides. EM simulation which includes dielectric losses is applied to get real filter response. The simulation values are optimized to set the desired result in filter response such as central frequency, insertion loss, and return loss.

After desired values are achieved in filter response with simulation, a designed parallel coupled microstrip bandpass filter is realized. The realized parallel coupled microstrip bandpass filter response is measured with a network analyzer. According to measurement results, it is decided to perform second realization to fix the deviation of central frequency in the first realization measurements. The designed filter is optimized

again to get the desired filter response and second realization is performed with new filter dimensions. In below, all the simulation process is defined with details.

Firstly, iFilter wizard is used to design a desired bandpass filter with central frequency 3.5 GHz and 200 MHz bandwidth. The output of simulator for even and odd mode impedance values are shown in below Figure 3.6. The calculated values in the previous section and simulator output values comparison are given in below Table 3.8. Calculated and simulation program values are close to each other.

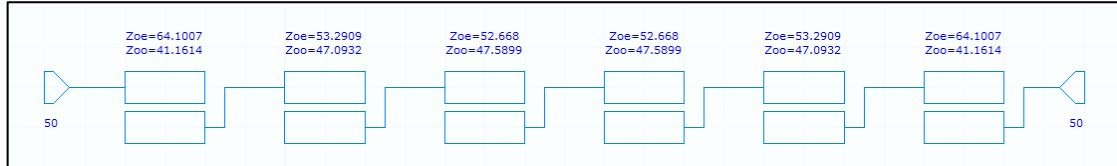


Figure 3.6 iFilter wizard even and mode values output for the desired filter

Table 3.8 Even and odd mode impedance values comparassion

Parallel Couple	Even Mode Impedance Z_e	Odd Mode Impedance Z_o	Even Mode Impedance iFilter Z_e	Odd Mode Impedance iFilter Z_o
1	64.10	41.16	64.10	41.16
2	53.29	47.09	53.29	47.09
3	52.66	47.58	52.66	47.58
4	52.66	47.58	52.66	47.58
5	53.29	47.09	53.29	47.09
6	64.10	41.16	64.10	41.16

From even and odd mode characteristic impedance values, the desired width, length and spacing of the strips are obtained by using the iFilter wizard built in AWR software. The values of resonator widths, lengths, and spacing between resonator couples which compose of bandpass microstrip filter are given in Table 3.9 and input and output 50 ohm strips width and length values in Table 3.10. The parallel coupled microstrip bandpass filter design layout and layout with dimensions are shown in Figure 3.7.

Table 3.9 Calculated dimensions of 3.5GHz bandpass filter

Line Description	Width W (mm)	Gap S (mm)	Length L (mm)
Coupled Line 1	0.982	0.373	13.119
Coupled Line 2	1.115	1.028	12.935
Coupled Line 3	1.118	1.149	12.928
Coupled Line 4	1.118	1.149	12.928
Coupled Line 5	1.115	1.028	12.935
Coupled Line 6	0.982	0.373	13.119

Table 3.10 Input and output 50 ohm line dimensions

	Width W (mm)	Length L (mm)
50 ohm line	1.133	6.611

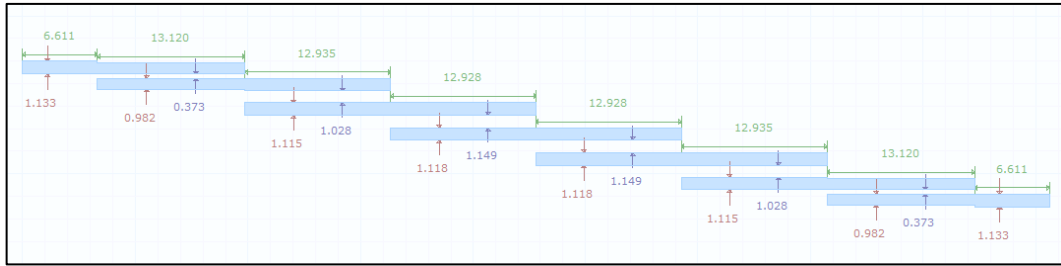


Figure 3.7 Filter layout

The calculated dimensions of the fifth (5th) order parallel coupled filter is compared with iFilter results. According to calculation limitations and simulation program advance iteration techniques, the difference is great between both results, very small changes in dimensions of microstrip filter are effected filter response in a great amount. In the simulation of bandpass filter using AWR software, EM simulation is applied to get dielectric losses into account (Dabhi & Dwivedi, 2016). In the remaining part of the filter design, the dimensions are calculated by iFilter. The dimensions of the designed filter are optimized to get the desired response according to filter response in simulation.

EM simulation is applied to the fifth (5th) order parallel coupled bandpass filter which is designed using by AWR iFilter wizard. In the filter, response bandwidth is less than the desired 200MHz when dielectric losses are taken into account. A new filter is designed with AWR iFilter wizard which response has approximately 200 MHz bandwidth after EM simulation is applied. In Figure 3.8, EM simulation filter response of the designed filter is shown.

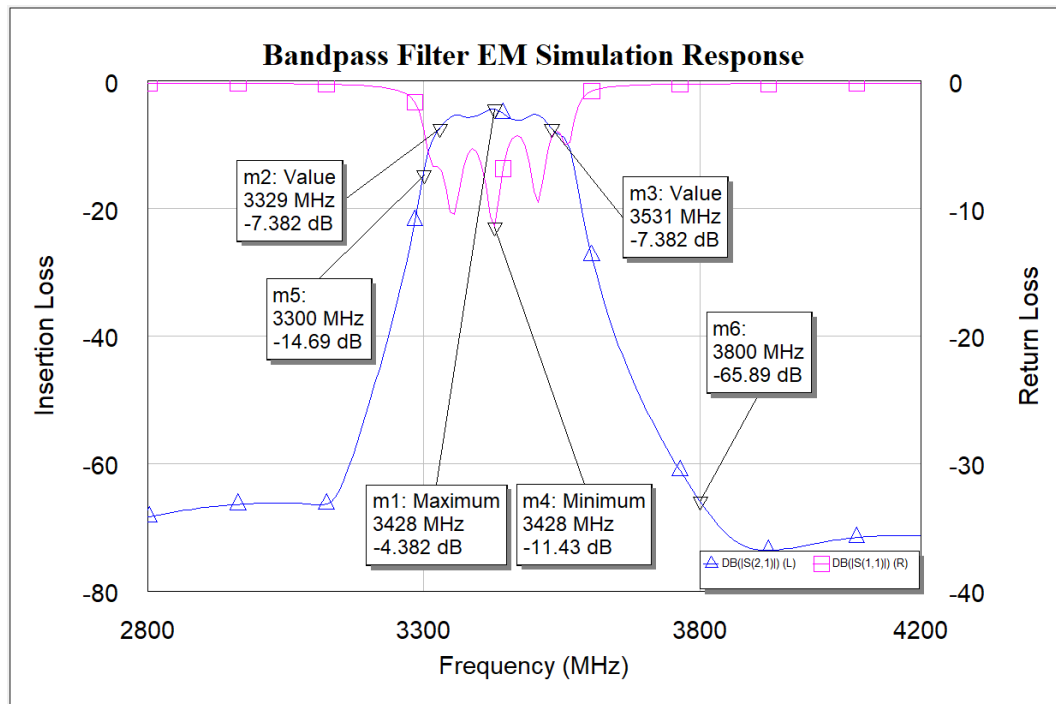


Figure 3.8 Bandpass filter EM simulation response

In Figure 3.8, bandpass filter response, insertion loss s_{21} is -4.382 dB, return loss s_{11} is -11.43 dB at 3428 MHz and -3 dB bandwidth is 202 MHz are shown.

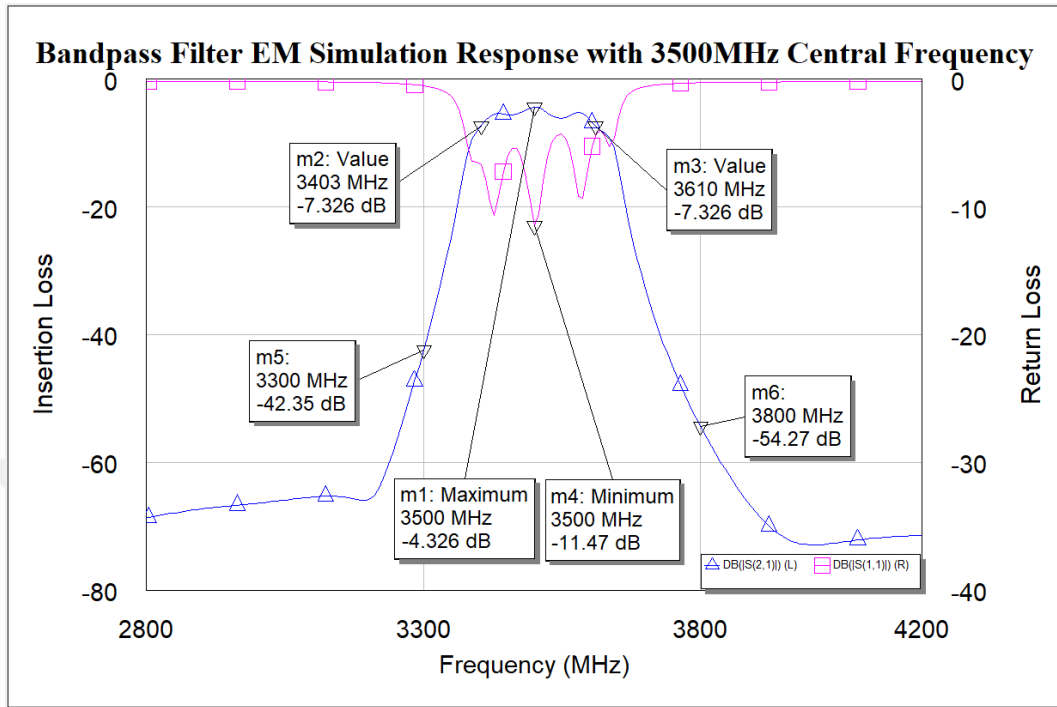


Figure 3.9 Bandpass filter EM simulation response with 3.5GHz central frequency

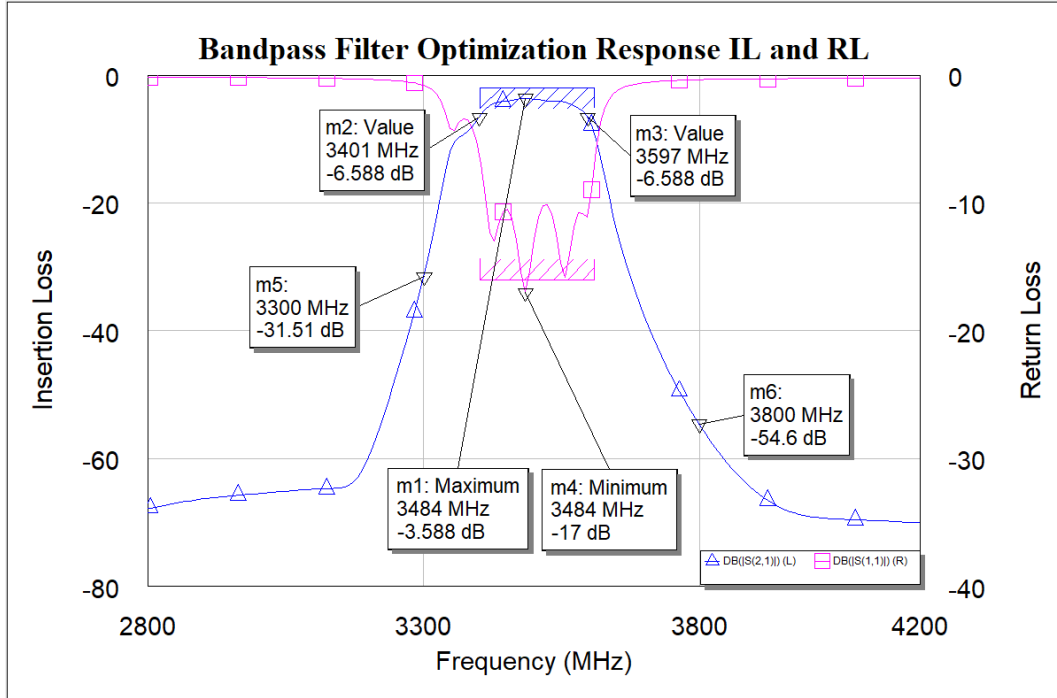


Figure 3.10 Bandpass filter optimization response IL and RL

After central frequency correction, to get better values as insertion loss and return loss in filter response, optimization goals are set as $IL > -2$ dB, $RL < -16$ dB and

optimization includes changing dimensions of resonators length, width, and spacing between resonator couples. Optimization is applied and new filter dimensions are defined as a result of optimization. In Figure 3.10, the filter response after optimization is applied is shown.

According to a shift in central frequency in the output of optimized filter response, resonators lengths are reduced again to set central frequency as 3.5 GHz. The circuit diagram of the designed filter in AWR software is given in Figure 3.11. The circuit diagram consist of elements blocks which are used for the notation of microstrips includes filter dimensions and substrate information. As a consequence of this optimization, in the Figure 3.12, the designed filter simulation result with new insertion loss s_{21} is -3.49 dB, return loss s_{11} is -16.94 dB at 3.5 GHz central frequency and -3 dB bandwidth is 199 MHz where upper and lower frequencies are 3617 MHz and 3418 MHz respectively are shown. The stopband attenuation at 3.8 GHz is -50.81 dB. The simulation results are met with filter specifications given at the beginning of the filter design. The filter layout before realization is given in the following Figure 3.13.

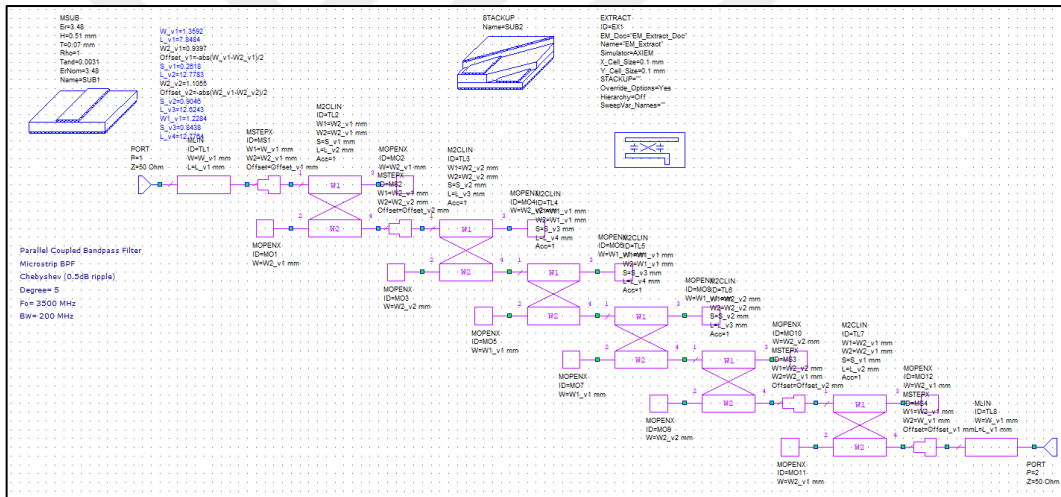


Figure 3.11 Circuit diagram of the designed bandpass filter.

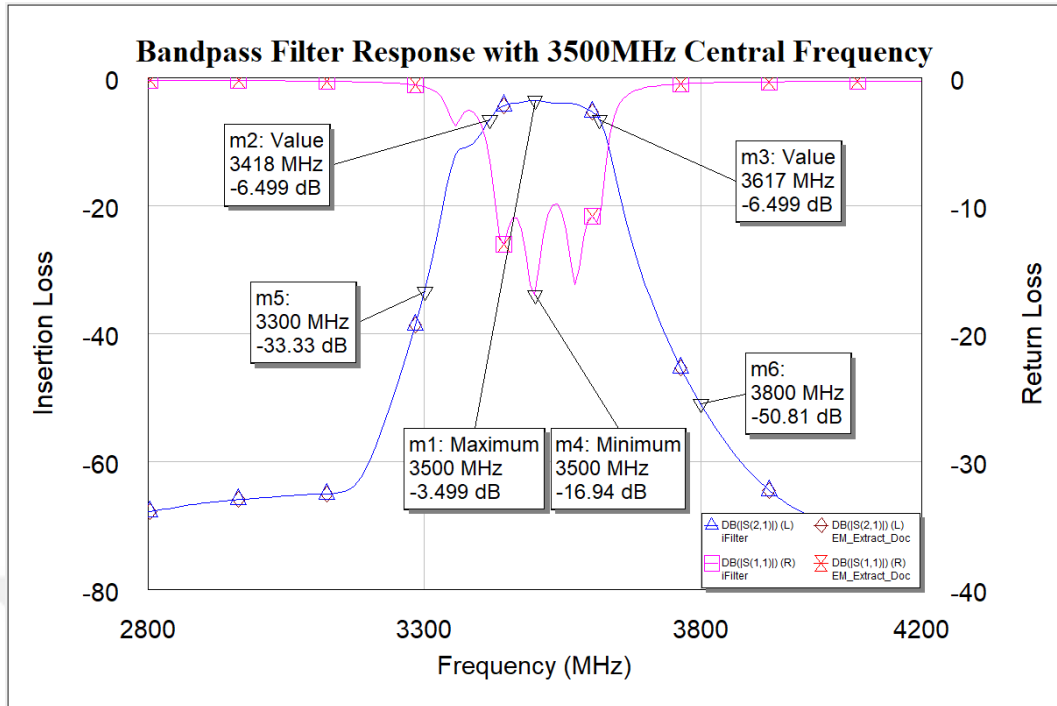


Figure 3.12 Bandpass filter response with 3.5 GHz central frequency.

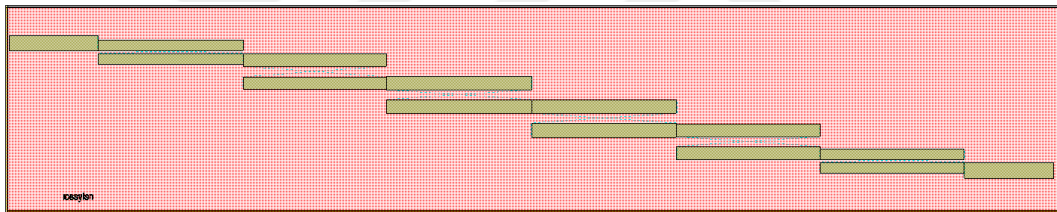


Figure 3.13 Microstrip filter layout.

The ultimate filter dimensions, filter designed and optimized filter are given in Table 3.11. Optimized filter dimensions are used for realization. The designed, simulated, and optimized filter layout is realized and measured. Optimized filter simulation response results and measured realized filter results are compared in the following section.

Table 3.11 Designed filter dimensions

Line Description	Filter Designed			Optimized Filter		
	W (mm)	S (mm)	L (mm)	W (mm)	S (mm)	L (mm)
50 ohm line input	1.133	-	6.611	1.359	-	7.848
Coupled Line 1	0.982	0.373	13.119	0.940	0.262	12.778
Coupled Line 2	1.115	1.028	12.935	1.106	0.905	12.624
Coupled Line 3	1.118	1.149	12.928	1.228	0.844	12.776
Coupled Line 4	1.118	1.149	12.928	1.228	0.844	12.776
Coupled Line 5	1.115	1.028	12.935	1.106	0.905	12.624
Coupled Line 6	0.982	0.373	13.119	1.940	0.262	12.778
50 ohm line output	1.133	-	6.611	1.359	-	7.848

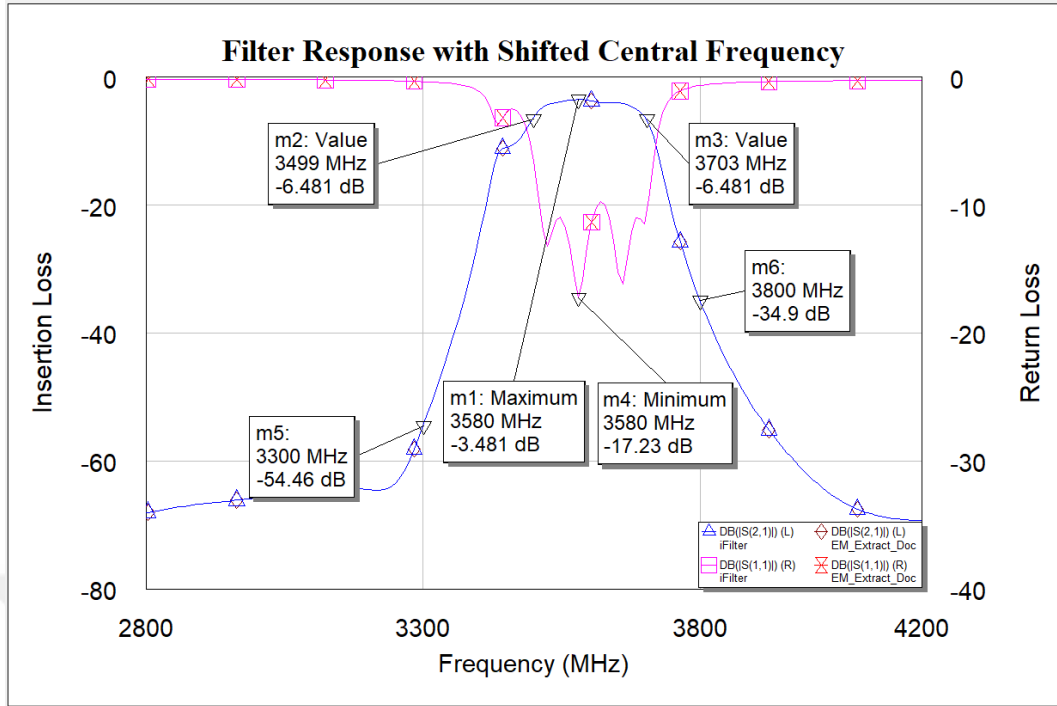


Figure 3.14 Filter response with shifted central frequency

The realized filter is measured and the filter response includes < %3 manufacturing error which causes central frequency shift to 3426 MHz from 3500 MHz. According to measurement results, to eliminate this error new design is applied for new realization which causes central frequency shift to the right from 3500 MHz to 3580 MHz in the simulation. The deviation from the central frequency in filter simulation is corrected by manufacturing error during realization and it is expected to be the central frequency of realized filter response will be measured as 3.5 GHz. In Figure 3.14, new designed filter simulation response which resonator lengths are reduced to move central frequency is shown.

The designed filter updated dimensions are given in Table 3.12. The parallel coupled microstrip bandpass filter new layout is created with new dimensions and shown in Figure 3.15.

Table 3.12 Filter layout dimensions

Line Description	Filter Dimensions		
	W (mm)	S (mm)	L (mm)
50 ohm line input	1.359	-	7.848
Coupled line 1	0.940	0.262	12.478
Coupled line 2	1.106	0.905	12.324
Coupled line 3	1.228	0.844	12.476
Coupled line 4	1.228	0.844	12.476
Coupled line 5	1.106	0.905	12.324
Coupled line 6	0.940	0.262	12.478
50 ohm line output	1.359	-	7.848

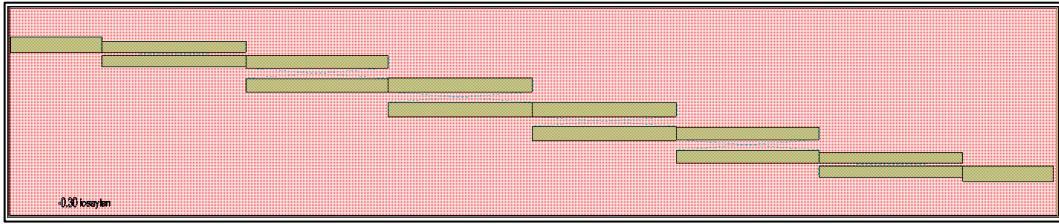


Figure 3.15 Microstrip filter new layout

The simulated filter new layout is realized and measured, both simulation and measured results are compared in the following section.

3.1.6 Measurement of Realized Design and Results

After the simulation part is completed, the realization of microstrip bandpass filter is performed to make the realization of the work. Realization of the designed parallel coupled microstrip bandpass filter is performed by a private and professional company to reduce manufacturing defects. The realized filter response measurements are performed at RF laboratory using a network analyzer.

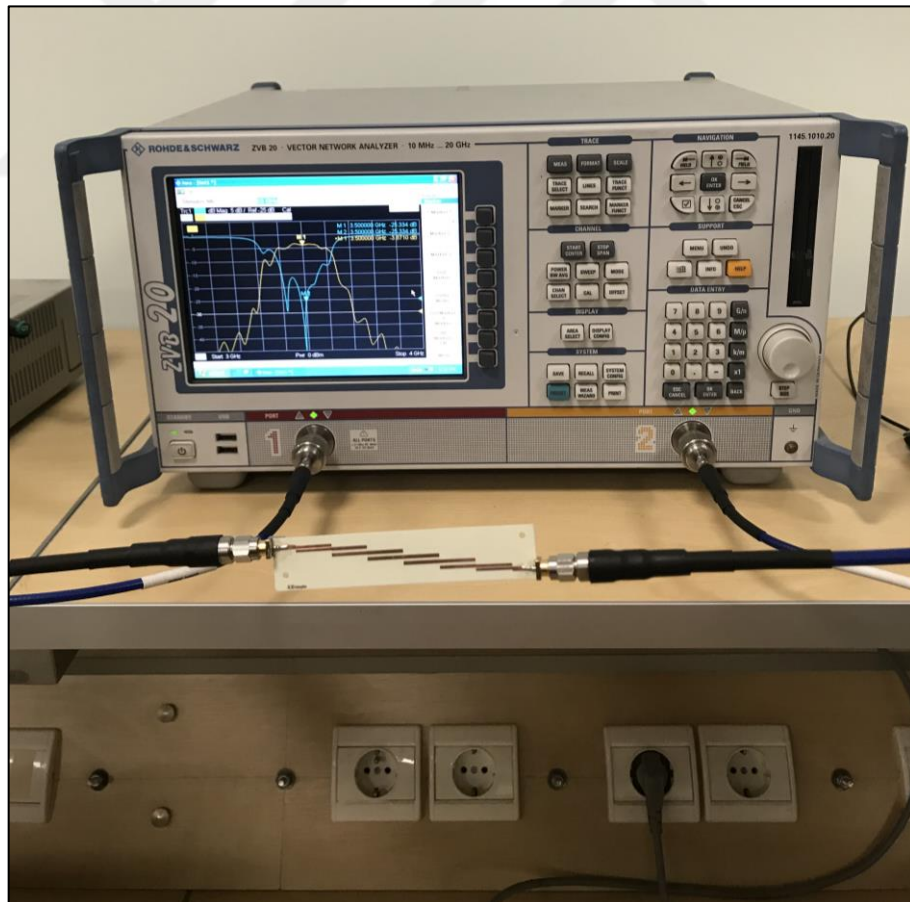


Figure 3.16 Measurement of realized filter with network analyzer

In Figure 3.17, filter response and some measurement values are given. The central frequency of the designed filter is shifted approximately 74 MHz to the left of simulation central frequency 3500 MHz to 3426 MHz. -3 dB bandwidth is 191 MHz with $f_1 = 3319$ MHz lower and $f_2 = 3510$ MHz upper cutoff frequencies. Stopband attenuation at 3800 MHz is -46.73 dB.

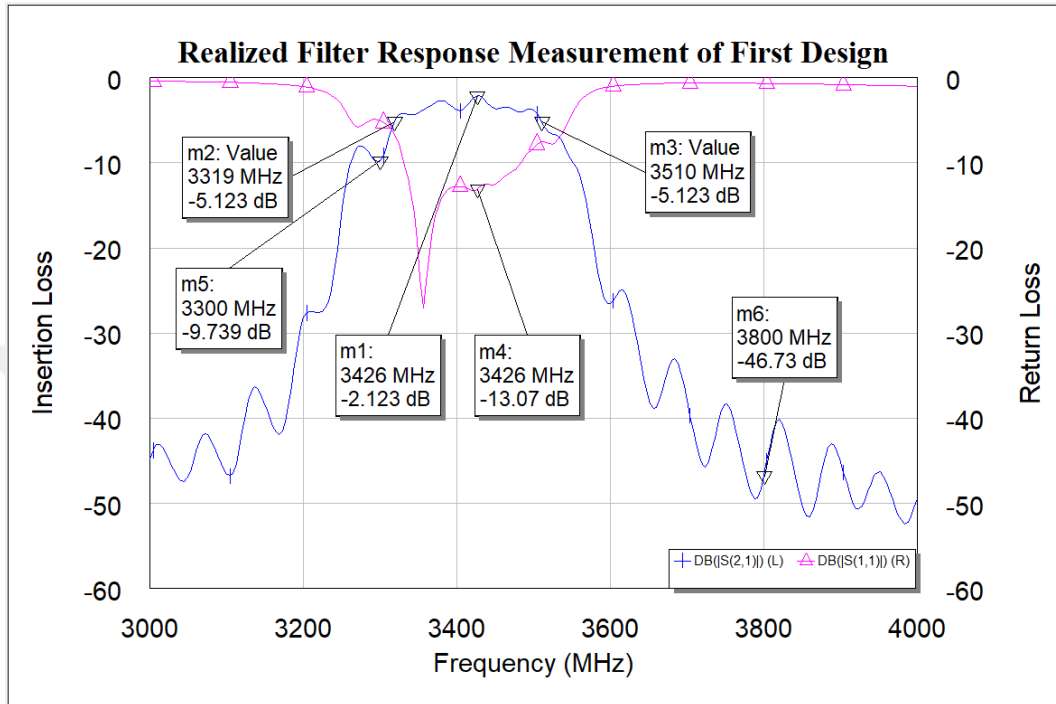


Figure 3.17 Realized filter response measurement of first design.

To make a realization much far better, this approximately $<3\%$ derivation in central frequency is taken into account and the second iteration is performed according to second simulation results. In Figure 3.18 realized parallel coupled microstrip bandpass filter with connected SMA connectors for measurement is shown. The newly realized filter is tested, response and some measurement values are given in Figure 3.19.



Figure 3.18 Parallel coupled microstrip bandpass filter

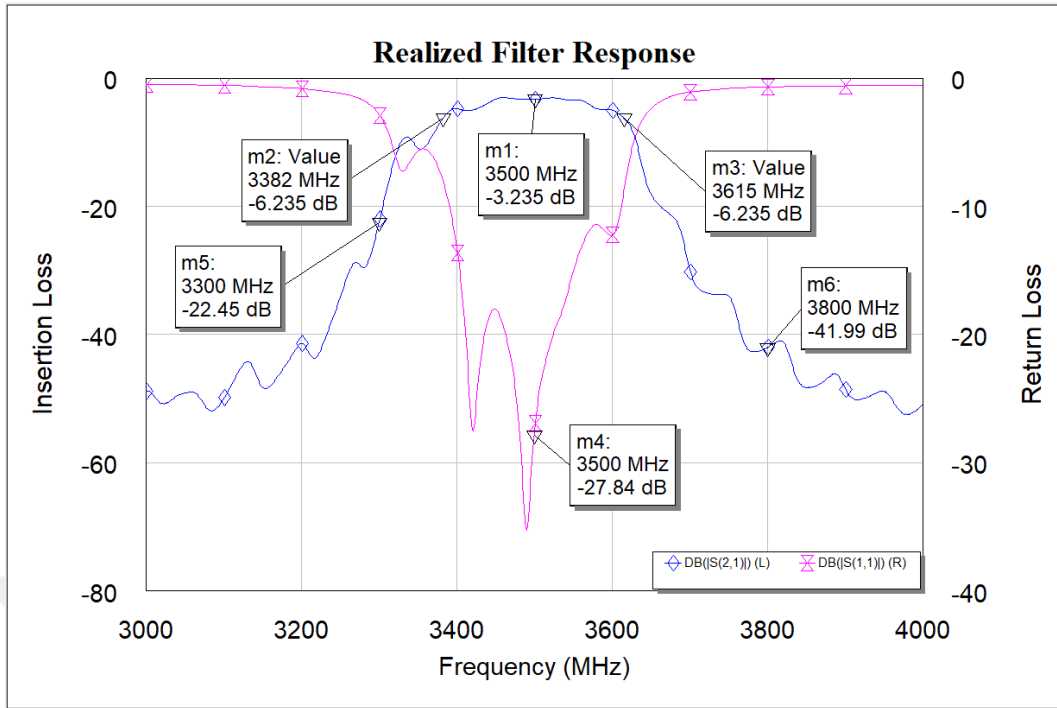


Figure 3.19 Realized filter response

The insertion loss s_{21} of the designed filter is $IL = -3.23$ dB and return loss s_{11} is $RL = -27.84$ dB at central frequency 3500 MHz. -3 dB bandwidth is 233 MHz with $f_1 = 3382$ MHz lower and $f_2 = 3615$ MHz upper cutoff frequencies. Stopband attenuation at 3800 MHz is -41.99 dB.

Table 3.13 shows both simulation results for the filter design and measured values of realized 5th order parallel coupled microstrip bandpass filter.

Table 3.13 Simulated and realized filter response values

Description	Simulated Filter Response	Realized Filter Response
Insertion Loss	-3.48 dB at 3580 MHz	-3.23 dB at 3500 MHz
Return Loss	-17.23 dB at 3580 MHz	-27.84 dB at 3500 MHz
Frequency Range (MHz)	3499 MHz to 3703 MHz	3382 MHz to 3615 MHz
Bandwidth (MHz)	204MHz	233MHz
Stopband Attenuation (dB)	-54.46 dB at 3300 MHz -34.09 dB at 3800 MHz	-22.45 dB at 3300 MHz -41.99 dB at 3800 MHz

SECTION 4. CONCLUSION

In some countries, 5G is started to use and its usage will be increased near future. One of the countries which started to deal with deployment 5G technology is the UK. In UK n78 (3300 MHz to 3800 MHz) band will be used for 5G applications. The 5G frequency band range is decided as between 3400 MHz to 3600 MHz in UK.

After the deployment of LTE in the UK, interference problem has emerged which effects tv broadcast. To prevent such problems, filters are designed to eliminate this interference between LTE and broadcast. The 5G frequency band n78 has adjacent bands used for a different type of applications. According to auction result in the UK, 3400 MHz to the 3600 MHz range is decided to use by telco operators. The filter design frequency range is selected as 3400 MHz to 3600 MHz because this range will be frequently used in the near future for NR 5G applications.

In this thesis, the 5th order parallel coupled microstrip bandpass filter with 3.5GHz central frequency and 200 MHz bandwidth are designed and simulated to eliminate interference to the 5G n78 band from adjacent bands. The filter is designed with 200 MHz bandwidth to cover all telco operator 5G applications bandwidths in the UK.

Before starting to filter design, literature are reviewed to improve knowledge about filter design, to examine existing works for filter design and to check upcoming and emerging new trends in frequency usage and new frequency allocation to use for communication. Initial filter design is started with using lumped-elements. Then, the transformation is applied to change lumped elements into distributed elements. Calculation is performed to calculate the lengths, widths of resonators and gaps between microstrip couples. Applied Wave Research (AWR) Design Environment software is used to make a simulation of calculated filter values. The filter design is continued with AWR software because of its high performance in iterative calculation during filter design. EM simulation main purpose is to find an approximate solution to Maxwell's equations which match a given set of boundary and initial conditions. In circuit simulation, signal flow is only through the connections that is draw between circuit components or blocks. In the block, coupling can be exist if the block includes coupled lines but for to take into account of coupling between blocks in the circuit EM simulation can be applied. In the designed filter coupling between coupled lines are also important, EM simulation is applied for this purpose and also to get dielectric losses into account. In the end, the filter is designed in the simulation program to meet design specifications. The layout file is created for realization and the design process is completed with the realization of microstrip parallel coupled line using the RO4350 substrate. Measurements are performed at the radio frequency (RF) laboratory using a network analyzer. The

realized filter response file is exported from the network analyzer and imported to AWR software to examine realized filter response.

As a result, to use a simulation program like AWR helps to decrease design periods and gain time to try different designs more rapidly because calculations take a much longer time. The simulation of the filter before realization helps to fix design mistakes beforehand, decrease wasting time and improve the design quality. Dielectric losses can get into account using EM simulation during filter design. Realized filter central frequency is deviated from simulation result so a new design is developed and simulated to eliminate this deviation. The second realized filter gives better results and meets the desired 3.5GHz central frequency in filter response. The insertion loss s_{21} is $IL = -3.23$ dB and return loss s_{11} is $RL = -27.84$ dB at a central frequency 3500 MHz, which meets the design specification. In the realized filter better insertion and return losses are achieved when compared with designed filter simulation response. -3 dB bandwidth is 233 MHz with 3382 MHz lower and 3615 MHz upper cutoff frequencies, it is quite a bit wider than desired 200 MHz in design specification but it is also in the range of n78 band (3300 MHz to 3800 MHz). Stopband attenuation at 3300 MHz is -22.45 dB which is decreased when compared to designed filter simulation response and at 3800 MHz is -41.99 dB which is better than designed filter simulation response. High stopband attenuation is achieved out of the n78 band as desired in design specifications. This high attenuation is blocked interference from adjacent bands.

In the Table 4.1, the designed filter specifications are compared with similar works. The designed and realized filter has good response results like low insertion loss, high return loss, high stopband attenuation, and low cost realization in comparison with some referanced works shown in the table. Despite the fact that the realized filter meets the specifications, the designed filter size is larger when compared other much more expensive used filter technologies like integrated circuit. But this loss in size can be ignored in the face of cheap costs depending on the application to be used.

Table 4.1 Comparison of designed filters

Reference	Order	Insertion Loss	Return Loss	Bandwidth	Stopband Attenuation	Technology	Dimensions
Realized filter in this thesis	5th	S_{21} – 3.23 dB at 3.5 GHz	S_{11} – 27.84 dB at 3.5 GHz	3382 MHz – 3615 Mhz 233 MHz	3300 MHz – 3800 Mhz > –22 dB & > –42 dB	Microstrip RO4350	9.21 cm x 1.23 cm
(Shin & Eilert, 2018)	-	< –1.8 dB	-	3300 MHz – 3800 Mhz 500 MHz	2700 MHz – 4900 Mhz > –30 dB	Silicon Integrated Passive Device (IPD)	-
(Nadera, Norhudah, & Tharek, 2015)	3rd	–1.53 dB	–15 dB	4750 MHz – 5250 Mhz 500 MHz	-	Microstrip RO4350	8.13 cm x 0.991 cm
(Vaghela, Sisodia, & Prabhakar, 2015)	3rd	–4.78 dB	–20.64 dB	2460 MHz – 2540 Mhz 80 MHz	at 2600 MHz –20 dB	Microstrip FR4 (h=1.2 mm, $\epsilon = 4.4$)	<9.136 cm x >1.194 cm
(Ferah & Jleed)	5th	–0.941 dB	–16.56 dB	2248 MHz – 2549 Mhz 301 MHz	-	Microstrip FR4 (h=1.58 mm, $\epsilon = 4.4$)	>9.136 cm x >1.194 cm
(Seghier, Benahmed, Bendimerad, & Benabdallah, 2012)	3rd	–0.914 dB	–19.31 dB	5900 MHz – 6100 Mhz 200 MHz	5600 MHz – 6200 Mhz –34.4 dB & – 15 dB	Microstrip RO4003C	<9.136 cm x <1.194 cm
(Arolkar & Virani, 2014)	3rd	–15 dB approx.	< –5 dB	2300 MHz 100 MHz	-	Microstrip FR4 (h=1.6 mm, $\epsilon = 4.4$)	<9.136 cm x <1.194 cm

New filters can be designed with different narrow bands like 50 MHz, 40 MHz or 20 MHz to match real single telco operator bandwidths or wide bandwidth like 500 MHz to cover all NR 5G n78 band (3.3 GHz to 3.8 GHz). Different microstrip topologies can be applied to decrease the size of the filter or to improve the performance of the filter. Better results can be achieved; by increasing order of filter but it will be cost to more area, by choosing another material with higher relative permittivity ϵ_r value but it will increase the price of a substrate. Wider resonators can be designed to decrease the length of filter but they require tightly coupled lines which is difficult to realize.

In the future, filter parts of communication systems will keep importance as like today, the increased demand of communication in every field of humans life will also cause to increase the demand and usage of the filter in applications. Frequency allocation will become more difficult with increasing communication demand. After LTE deployment in the UK, the frequency used for LTE caused interference between LTE and TV broadcast. To prevent from interference problems in advance, upcoming technologies can be followed and new filter designs can be performed beforehand.



REFERENCES

- Abbas, T., Ahmed, Z., & Ihsan, M. B. (2004). Parallel Coupled Microstrip Band Pass Filter Design using EM-Analysis. *8th International Multitopic Conference, 2004. Proceedings of INMIC 2004*. Lahore, Pakistan: IEEE.
- Abbas, T., Zubair, A., & Mojeeb, B. I. (n.d.). Parallel Coupled Microstrip Band Pass Filter Design using EM-Analysis. *IEEE International Multi-topic Conference*, 703-705.
- Akhtarzad, S., Rowbotham, T. R., & Johns, P. B. (1975, June). The Design of Coupled Microstrip Lines. *IEEE Transactions on Microwave Theory and Techniques*, *MTT-23*(6), 486-492.
- Al-Areqi, N. N., Seman, N., & Rahman, T. A. (2017). Design of Microstrip Parallel-Coupled Line Band Pass Filters for the Application in Fifth-Generation Wireless Communication. *Journal of Telecommunication, Electronic and Computer Engineering (JTEC)*, *9*(2-7), 19-23.
- Albreem, M. A. (2015). 5G Wireless Communication Systems: Vision and Challenges. *International Conference on Computer, Communication, and Control Technology (I4CT 2015)* (pp. 493-497). Kuching, Sarawak, Malaysia: IEEE.
- Arolkar, R., & Virani, D. (2014, February). Design of Microstrip Bandpass Filter at 2.3 GHz. *International Journal for Research in Technological Studies*, *1*, 59-61.
- Bahl, I., & Trivedi, D. (1977, May). A Designer's Guide to Microstrip Line. *Microwaves*, 174-182.
- Barrett, R. M. (1984, September). Microwave Printed Circuits—The Early Years. *IEEE TRANSACTIONSON MICROWAVETHSORYAND TECHNIQUE*, *32*, 983-990.

- Bhattacharjee, A., & Singh, N. K. (2012). Design, Fabrication And Analysis of Parallel-Coupled Line Bandpass Microstrip Filter for C-Band Application. *International Journal of Electrical, Electronics and Computer Engineering*, 51-54.
- Çakır, G., Gündüz , S., & Sevgi, L. (2006). *Geniş Bantlı Mikroşerit Filtre Tasarımı*. İstanbul: Eksen Yayıncılık.
- Cheng, D. K. (1992). *Field and Wave Electromagnetics*. Addison - Wesley Publishing Company Inc.
- Collin, R. E. (2001). *Foundations for microwave engineering* (2nd ed.). Hoboken, New Jersey: John Wiley & Sons, Inc.
- Cristal, E. G. (1975, December). Tapped-Line Coupled Transmission Lines with Applications to Interdigital and Compline Filters. *IEEE TRANSACTIONS ON MICROWAVE THEORY AND TECHNIQUES*, 1007-1012.
- Dabhi, V. M., & Dwivedi, V. V. (2016). Parallel Coupled Microstrip Bandpass Filter Designed and Modeled at 2 GHz. *International conference on Signal Processing, Communication, Power and Embedded System (SCOPEs)*, 461-466.
- Dishal, M. (1965). A simple design procedure for small percentage bandwidth round-rod interdigital filters. *IEEE transactions on microwave theory and techniques*, 696-698.
- Edwards, T. C., & Steer, M. B. (2016). *Foundations for Microstrip Circuit Design*. John Wiley & Sons, Ltd.
- Eroglu, A., & Lee, J. K. (2008). The Complete Design of Microstrip Directional Couplers Using the Synthesis Technique. *IEEE TRANSACTIONS ON INSTRUMENTATION AND MEASUREMENT*, 2756-2761.
- Ferh, A. E., & Jleed, H. (n.d.). Design, Simulate and approximate Parallel Coupled Microstrip BandPass Filter at 2.4 GHz.

- Floyd, T. L. (2012). *Electronic Devices : conventional current version* (Vol. 9th ed.). New Jersey: Prentice Hall.
- Gupta, K. c., Garg, R., Bahl, I., & Bhartia, P. (1996). *Microstrip Lines and Slotlines* (2nd ed.). Boston: Artech House.
- Hammerstad, E. O. (1975). Equations for microstrip circuit design. *European Microwave Conference* (pp. 268-272). Hamburg: Proceedings of the European Microwave Conference.
- Hammerstad, E. O., & Bekkadal, F. (1975). *Microstrip Handbook*. Trondheim: Electronics Research Laboratory, University of Trondheim, Norwegian Institute of Technology .
- Hinton, J. H. (1980). On Design of Coupled Microstrip Lines. *IEEE Transactions on Microwave Theory and Techniques, MTT-28*, 272.
- Hong, J. S., & Lancaster, M. J. (2001). *Microstrip Filters for RF/Microwave Applications*. John Wiley & Sons Inc.
- Kirschning, M., & Jansen, R. H. (1984, January). Accurate Wide-Range Design Equations for the Frequency-Dependent Characteristic of Parallel Coupled Microstrip Lines. *IEEE Transactions on Microwave Theory and Techniques, MTT-32*(1), 83-90.
- Levy, R., Snyder, R. V., & Matthaei, G. (2002, March). Design of Microwave Filters. *IEEE TRANSACTIONS ON MICROWAVE THEORY AND TECHNIQUES*, 50(3), 783-793.
- Ludwig, R., & Bretchko, P. (2000). *RF Circuit Design Theory and Applications*. New Jersey: Prentice Hall Inc.
- Mahon, S. (2017, November). The 5G Effect on RF Filter Technologies. *TRANSACTIONS ON SEMICONDUCTOR MANUFACTURING*, 494-499.

- Mariani, E. A., & Agrios, J. P. (1970). Slot-Line Filters and Couplers. *IEEE TRANSACTIONS ON MICROWAVE! THEORY AND TECHNIQUES*, 18, 1089-1095.
- Matthaei, G. L., Young, L., & Jones, E. T. (1980). *Microwave Filters, Impedance-Matching Networks, and Coupling Structures*. Norwood, MA: Artech House, Inc.
- Microwave Journal*. (2019, 03 16). Retrieved from <https://www.microwavejournal.com/blogs/1-rog-blog/post/18978-choose-circuit-materials-for-bandpass-filters>
- Mongia, R. K., Bahl, I. J., Bhartia, P., & Hong, J. (2007). *RF and Microwave Coupled-Line Circuits* (2nd ed.). Norwood.
- Nadera, N. A.-A., Norhudah, S., & Tharek, A. R. (2015). Parallel-Coupled Line Bandpass Filter Design Using Different Substrates for Fifth Generation Wireless Communication Applications. *ISAP2015*.
- Othman, M. A., Sinnappa, M., Hussain, M. N., Aziz, M. A., & Ismail, M. M. (2013, Aug-Sep). Development of 5.8 GHz Microstrip Parallel Coupled Line Bandpass Filter for Wireless Communication System. *International Journal of Engineering and Technology (IJET)*, 5(4), 3227-3235.
- Pozar, D. M. (2012). *Microwave Engineering*. John Wiley & Sons Inc.
- Richard, P. I. (1948). Resistor-Transmission-Line Circuits. *Proceedings of the I.R.E.*, 217-220.
- Rohde, U. L., & Newkirk, D. P. (2000). *RF/MICROWAVE CIRCUIT DESIGN FOR WIRELESS APPLICATIONS*. New York: John Wiley & Sons, Inc.
- Schaumann, R., & Van Valkenburg, M. E. (2001). *Design of Analog Filters*. Oxford University Press.
- Seghier, S., Benahmed, N., & Benabdallah, N. (n.d.). Design of Parallel Coupled Microstrip Bandpass Filter for FM Wireless Applications.

- Seghier, S., Benahmed, N., Bendimerad, F. T., & Benabdallah, N. (2012). Design of Parallel Coupled Microstrip Bandpass Filter for FM Wireless Applications. *6th International Conference on Sciences of Electronics, Technologies of Information and Telecommunications (SETIT)*. Sousse, Tunisia: IEEE.
- Shin, K. R., & Eilert, K. (2018). Compact Low Cost 5G NR n78 Band Pass Filter with Silicon IPD Technology. *19th Wireless and Microwave Technology Conference (WAMICON)*. Sand Key, FL, USA: IEEE.
- Srinath, S. (2014, June). Design of 4th Order Parallel Coupled Microstrip Bandpass Filter at Dual Frequencies of 1.8 GHz and 2.4 GHz for Wireless Application. *International Journal of Innovative Research in Computer and Communication Engineering*, 2(6), 4744-4751.
- Tsai, C.-M. (2007, April). Improved Design Equations of the Tapped-Line Structure for Coupled-Line Filters. *MICROWAVE AND WIRELESS COMPONENTS LETTERS*, 17(4), 244-246.
- Vaghela, D. V., Sisodia, A. K., & Prabhakar, N. M. (2015). Design, Simulation and Development of Bandpass Filter at 2.5 GHz. *International Journal of Engineering Development and Research*, 1202-1209.
- Vipul, M. D., & Ved, V. D. (2016). Parallel Coupled Microstrip Bandpass Filter Designed and Modeled at 2 GHz. *International conference on Signal Processing, Communication, Power and Embedded System (SCOPE5)*, 461-466.
- Wadell, B. C. (1991). *Transmission Line Design Handbook*. Norwood, MA: Artech house, Inc.
- WEN, C. P. (1969, December). Coplanar Waveguide: A Surface Strip Transmission Line Suitable for Nonreciprocal Gyromagnetic Device Applications. *IEEE TRANSACTIONS ON MICROWAVE THEORY AND TECHNIQUES*, MTT-17, 1087-190.
- Wong, J. S. (1979). Microstrip Tapped-Line Filter Design. *IEEE Transactions on Microwave Theory and Techniques*, MTT-27, 44-50.

Yang, S., Cross, D., & Drake, M. (2014). Design and Simulation of a Parallel-Coupled Microstrip Bandpass Filter.

Internet References

(URL-1, 2018), http://www.3gpp.org/ftp//Specs/archive/38_series/38.104/, Retrieved: 01 16. 2019.

(URL-2, 2018), https://www.ofcom.org.uk/__data/assets/pdf_file/0017/112931/2.3-GHz-and-3.4-GHz-band-plans-based-on-final-auction-results.pdf, Retrieved: 01 16. 2019.



